STUDIES ON FRACTAL MICROSTRIP ANTENNA ARRAYS FOR WIRELESS MIMO APPLICATIONS

A Thesis Submitted in Partial Fulfillment of the Requirement for the Award of the Degree of

MASTER OF ENGINEERING

in

Wireless Communication Engineering

Submitted by

JAIVINDER SINGH

801663002

Under the Supervision of

Dr. Amanpreet Kaur

Assistant Professor, ECED

ELECTRONICS AND COMMUNICATION ENGINEERING DEPARTMENT

THAPAR INSTITUTE OF ENGINEERING AND TECHNOLOGY

(A DEEMED TO BE UNIVERSITY) PATIALA, PUNJAB

JULY, 2018

DECLARATION

I, **Jaivinder Singh**, hereby declare that the work presented in this thesis entitled "**STUDIES ON FRACTAL MICROSTRIP ANTENNA ARRAYS FOR WIRELESS MIMO APPLICATIONS**" in the partial fulfilment of the requirement for the award of degree of Master of Engineering (Wireless Communication) submitted in Electronics and Communication Engineering Department, Thapar Institute of Engineering & Technology (T.I.E.T., Deemed University), Patiala, India is an authentic record of my own work carried out under the supervision/guidance of **Dr. Amanpreet Kaur** (Assistant Professor), Electronics and Communication Engineering Department, T.I.E.T., Patiala from Jan 2017 to July 2018.

The matter presented in this thesis has not been submitted either in part or full to any other university or institute for the award of any other degree.

Date: 13/07/2018

Jaivinder Singh

Roll No: 801663002

It is certified that the above statement made by the candidate is correct to the best of my knowledge and belief.

Date: 13/07/2018

Dr. Amanpreet Kaur 13.7.18

Assistant Professor, ECED

T.I.E.T., Patiala, Punjab, India

ACKNOWLEDGEMENT

First of all, I express my sincere thanks to the all almighty GOD for honouring me with knowledge, intelligence, well-being, cognizance and the brainpower to conduct this research successfully.

I wish to express my deep gratitude and sincere thanks to my supervisor, **Dr. Amanpreet Kaur**, Assistant Professor, Electronics and Communication Department (ECED), T.I.E.T., Patiala, for her invaluable guidance, constant encouragement, constructive comments, sympathetic attitude, and immense motivation, which has sustained my efforts at all stages of this work. Her valuable advice and suggestions for the corrections, modifications and improvement did enhance my work.

I would like to express my gratitude to **Dr. Alpana Agarwal**, the Head of Electronics and Communication Department (ECED), T.I.E.T., Patiala, for providing me with adequate environment in carrying out the work. I am also thankful to the program coordinator, **Dr. Ashutosh Kumar Singh**, Electronics and Communication Engineering Department (ECED) for his constant guidance about the thesis work.

Finally, I want to extend my gratitude to all those persons who directly or indirectly helped me in carrying out this work in right direction.

Jaivinder Singh

ABSTRACT

As the world is moving very fast in the perspective of technology, wireless communication plays a vital role in the making a better future. Antennas are the devices by which we can transfer the data wirelessly. There are many types of antennas with different shapes and sizes. Nowadays every modern wireless equipment is implemented with Wi-Fi (Wireless WLAN), Bluetooth and many more such technologies. For the same we need broadband and multi-band antennas to cover the various applications in a same terminal device. In order to have better transmitting and receiving rate broadband antennas are required. In addition, for miniaturising the wireless communication system, the antennas must be small enough to be placed inside the system. The microstrip antennas have various advantages that make them a good candidate for their use in the current wireless communication systems.

The main focus nowadays is to increase the speed of the data communication in the antenna with minimum noise, so MIMO antennas came into being. Therefore the research work presented in this thesis concentrates on the study of fractal aperture coupled microstrip antenna arrays that can be used in the MIMO systems. The research work starts with firstly designing a simple aperture coupled square patched antenna with edges sliced which covers a bandwidth of 139.4 MHz from 2.364 GHz to 2.5034 GHz. Then a sierpinski gasket fractal antenna and hexagonal antenna with defected ground structure and aperture coupling is designed which is then converted into 2x2 MIMO antenna and these cover a bandwidth of 1.006 GHz from 5.4832 GHz to 6.4892 GHz for a 2x2 MIMO array.

Secondly, a hexagonal antenna with defected ground structure and aperture coupling is designed. This shows dual-band behaviour for frequencies between (5.139-5.274) GHz and (8.71-9.44) GHz for WLAN and X-band applications. It is also converted to an array with two antennas and can be used for a 2x2 MIMO antenna array. The research work is then extended to surface capable of allowing particular range of frequency and rejecting all other unwanted frequencies. An antenna based on FSS is also designed to provide selective band behaviour from the antenna. In this thesis the FSS based antennas focuses on the implementation of a bandstop filter from 8 GHz to 10 GHz and covering a dual band from (3.67-3.75) GHz and (6.44-7.88) GHz. This designed antenna is suitable for IEEE 802.11, C-band, X-band applications.

Lastly two fabricated antennas i.e. 2x2 triangular sierpinski gasket fractal antenna and hexagonal antenna with defected ground structure are tested using VNA to validate the results. The tested results and the comparison of tested and simulated results are also shown. A good match between the simulated and tested results allows the antenna to be suitable for desired wireless applications.

TABLE OF CONTENTS

LIST OF TABLES

LIST OF FIGURES

LIST OF ABBREVIATIONS

ACO	Ant Colony Optimization
CASA	Circular Aperture Slot Antenna
CM	Common Mode
CP	Circular Polarization
CPW	Coplanar Waveguide
CST-MWS	Computer Simulation Technology Microwave Studio
dBi	Decibel Isotropic
DCS	Distributed Control System
DG	Defected Ground
DGS	Defected Ground Structure
DMS	Defected Microstip Structure
DOA	Direction Of Arrival
DSP	Digital Signal Processor
EBG	Electromagnetic Bandgap
ECC	Envelope Correlation Coefficient
EGC	Equal Gain Combining
EM	Electromagnetic Wave
FSS	Frequency Selective Surface
GHz	Gigahertz
GPS	Global Positioning System
LHCP	Left Hand Circular Polarisation
LMS	Least Mean Square
LTE	Long Term Evolution
MAFSS	Multifunctional Active Frequency Selective Surface
MEMS	Micro-Electro Mechanical System
MFSS	Multifunction Frequency Selective Surface
MHz	Megahertz

MIMO	Multi Intput Multi Output
MRC	Maximum Ratio Combining
MSA	Microstrip Antenna
OC	Open Circuit
PCS	Personal Communication System
RF	Radio Frequency
RFID	Radio Frequency Identification
RHCP	Right Hand Circular Polarisation
SC	Selection Combining
SISO	Single Input Single Output
SLL	Side Lobe Level
SNR	Signal to Noise Ratio
TE	Transverse Electric Mode
TEM	Transverse Magnetic Waves
TM	Transverse Magnetic
UMTS	Universal Mobile Telecommunication System
UWB	Ultrawide Band
VNA	Voltage Standing Wave Ratio
VSWR	Voltage Standing Wave Ratio
Wi-Fi	Wireless Fidelity
Wi-BRO	Wireless Broadband
WiMAX	Worldwide Interoperability for Microwave Access
WLAN	Wireless Local Area Network

CHAPTER 1

INTRODUCTION

1.1 OVERVIEW

With the modernization of technology, wireless communication systems have grown rapidly. Antenna forms an inevitable part of any wireless communication system. Antenna is an electrical device which transmits the electromagnetic waves into the space by converting the electric power given at the input into the radio waves and at the receiver side the antenna intercepts these radio waves and converts them back into the electrical power [1]. There are a number of systems that use antennas such as remote controlled television, cellular phones, satellite communications, spacecraft, radars, wireless phones and wireless computer networks. Day by day new wireless devices are introducing with increasing demands of compact antennas. Increase in the satellite communication and use of antennas in the aircraft and spacecraft has also increased the demands of low profile antennas that can provide a reliable communication [2].

A microstrip antenna offers a low profile and is light weighted. It is narrowband antenna & can be manufactured easily by the printed circuit technology such as a metallic layers in a particular shape is bonded on a dielectric substrate which forms a radiating element and another continuous metallic layer on the other side of substrate as ground plane. Not only the basic shapes, any continuous shape can be used as the radiating patch. Figure 1.1 shows the basic geometry of a MSA. Instead of using dielectric substrate some of the microstrip antennas use dielectric spacers which results in wider bandwidth but in the cost of less ruggedness. The size of microstrip antenna is related to the wavelength of operation generally $\lambda/2$ [1]. The applications of microstrip antennas in the microwave frequency band is preferred because of the size issues of the antenna at lower frequencies. Nowadays microstrip antenna is used in commercial sectors due to its inexpensiveness and easy to manufacture benefit by using advanced printed circuit technology. Due to the development and ongoing research in the area of microstrip antenna it is expected that in future most of the conventional antennas will be replaced by microstrip antennas [1].

In order to improve the signal to noise ratio & thus offer an increased data rate, the current wireless systems are using many diversity schemes. Here multiple antennas are required at the transmitter/receiver side to implement these diversity schemes. Such systems that use multiple antennas at Tx/Rx side are called MIMO systems and are explained in detail in the next section.

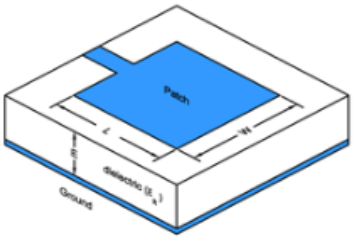

Figure 1.1 Microstrip patch antenna [2]

1.2 MIMO ANTENNA'S

MIMO or multi-input multi-output is a RF technology which is being used in many wireless technologies like LTE or long term evolution, Wi-Fi etc. which provides better link capacity and spectral efficiency than basic SISO or single-input single-output antenna. Figure 1.2 shows a basic MIMO wireless communication system. Here multiple antennas are installed at the transmitter as well as receiver side to be used with a specific diversity scheme like the MRC (Maximum ratio combining), EGC (Equal gain combining), SC (Selection combining) in order to improve the signal to noise ratio to get a better signal quality at the receiver even with low transmitted power [4].

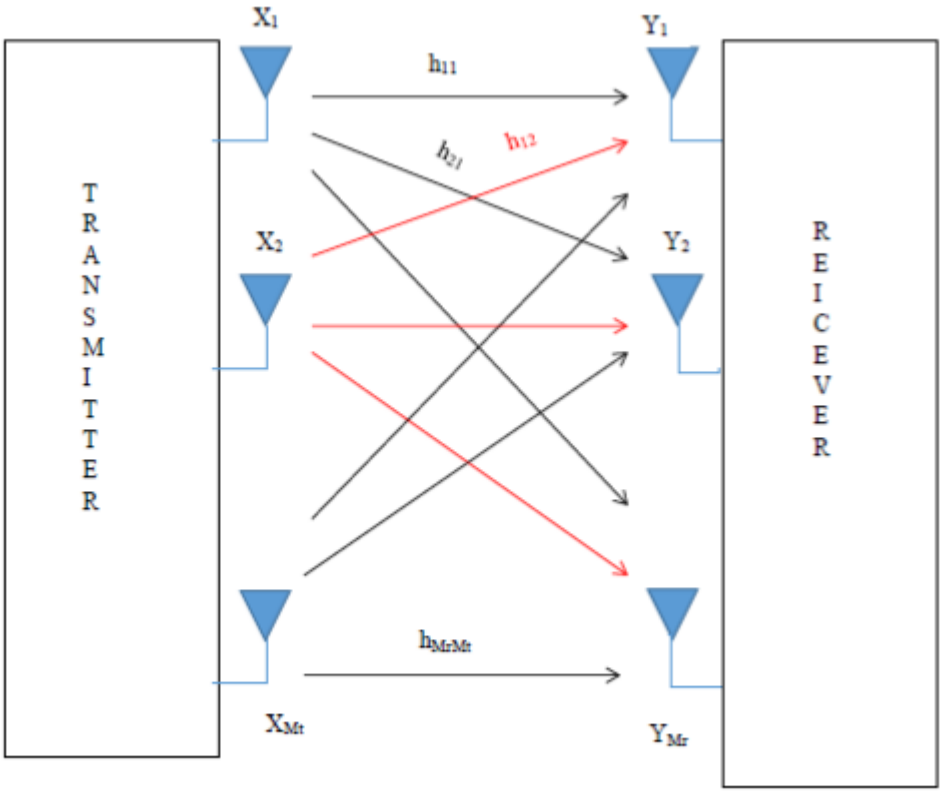

Figure 1.2 MIMO Architecture [3]

$$Y = HX \tag{1.1}$$

$$H_{(i,j)} = \begin{bmatrix} h_{1,1} & h_{1,2} & \cdots & h_{1,M_T} \\ h_{2,1} & h_{2,1} & \cdots & h_{2,M_T} \\ \vdots & \vdots & \ddots & \vdots \\ h_{M_R,1} & h_{M_R,2} & \dots & h_{M_R,M_T} \end{bmatrix} \tag{1.2}$$

Equations 1.1 and 1.2 represent the H matrix of the above shown MIMO system. The capacity of the system increases linearly with the minimum number of antenna deployed at the transmitting and the receiving side. In the Figure1.2 $X(X_1, X_2 \dots . X_{M_T})$ is the transmitted signal and $Y(Y_1, Y_2 \dots . Y_{M_R})$ is the

signal received by the receiver and $H_{(i,j)}$ represents the channel matrix given in equation 1.2. H matrix is used to estimate the channel by which the received signal is estimated.

where, i=Receiving antenna, j= Transmitting antenna

1.2.1 MIMO Antenna Parameters

Antenna parameters that are used to judge the quality of a MIMO system such as ECC, diversity gain and array gain are discussed below

- **Envelope Correlation Coefficient (ECC)**

  Envelope Correlation Coefficient tells us how independent two antennas' radiation patterns are. So if one antenna is completely horizontally polarized, and the other is completely vertically polarized, the two antennas would have a correlation of zero. Similarly, if one antenna only radiated energy towards the sky, and the other only radiated energy towards the ground, these antennas would also have an ECC of 0. Hence, Envelope Correlation Coefficient takes into account the antennas' radiation pattern shape, polarization, and even the relative phase of the fields between the two antennas. Equation 1.3 gives ECC for a 2x2 MIMO antenna array.

$$ECC = \frac{|S_{11}^{*}S_{22}+S_{21}^{*}S_{12}|^{2}}{(1-|S_{11}|^{2}-|S_{21}|^{2})(1-|S_{22}|^{2}-|S_{12}|^{2})} \quad (1.3)$$

- **Array Gain**

  It can be defined as the average increase in the signal to noise ratio present at the receiver arising from the coherent combination of multiple antennas. The signals that arrive at the receive antenna have different amplitudes and phases. The receiver then combines the received signals coherently which enhances the resultant signal. This results in improved reliability, and the capacity of the system.

- **Spatial Diversity gain**

  When signal power drops notably the channel is said to be suffering with a fade. Diversity schemes like MRC, EGC, SC and OC are used to nullify fading. Spatial diversity makes the use of independent copies of the transmitted signal at the receiver. In this scheme the rich scattering nature of the channel is exploited, hence the probability of all the transmitted signals undergoing deep fade becomes very less.

$$DG = 10\sqrt{1-(ECC)^{2}} \quad (1.4)$$

The initial work on MIMO systems focussed on basic spatial diversity - here the MIMO system was used to limit the degradation caused by multipath propagation. However this was only the first step as system then started to utilise the multipath propagation to advantage, turning the additional signal paths into what might effectively be considered as additional channels to carry additional data [4].

With microstrip antennas, MIMO structures can be implemented easily. Instead of one radiating patch and feed line the Tx/Rx can have 2 or 4 antennas printed on the same substrate making it an array. These structures repeated which can work as MIMO antennas but the distance between the radiating patch should be n*λ/2 so that they don't interfere with each other's radiation. For successful operation of this array, the correlation factor ECC should be less than 0.5 in order to provide a good diversity gain of around 9 or more.

Since MSA are the antennas of future because of their inherent advantages, next section focuses on MSA, its operation mechanism & feeding methods.

1.3 MICROSTRIP PATCH ANTENNAS

Microstrip patch antennas are becoming very popular now days as they can be printed directly onto a circuit board and can be placed where the space is little that's why they are becoming widespread within the mobile phone market. They are easily fabricated and have low cost as compared to other antennas. Basic microstrip patch antenna (as shown in figure 1.3) consists of a patch having length L, width W and some height h which rests on a substrate with ground plane and the feed line. Patch, ground plane and transmission line are made up of high conductive metal mostly cooper and the substrate is made up of dielectric material with permittivity ε_r.

1.3.1 Transmission Line Model

This model represents the microstrip antenna by two slots of width W and height h, separated by a transmission line of length L. The microstrip is essentially a non – homogenous line of two dielectrics, typically the substrate and air. As a result, this transmission line cannot support pure transverse electric magnetic (TEM) mode of transmission, since the phase velocities would be different in the air and the substrate. The value of ε_{reff} is slightly less than ε_r because the fringing fields around the periphery of the patch are not confined in the dielectric substrate but are also spread in the air [5, 6 and 7].

In applying the transmission line model, the following calculation steps are used to determine the required parameters for a patch antenna.

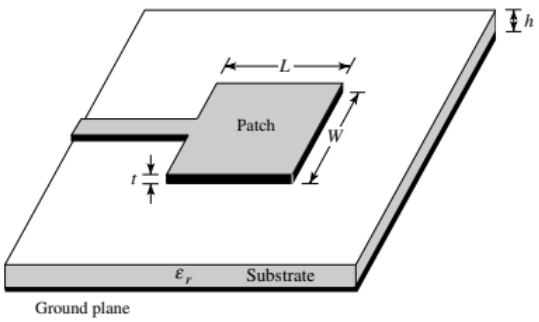

Figure 1.3 Illustration of patch antenna dimensions [2]

- Calculation of the antenna width (W): Having specified the height of the patch antenna, the first step in the design procedure is to determine the width of the patch. This can be calculated using the following equation;

$$w = \frac{c}{2f_{\circ}\sqrt{\frac{(\varepsilon_r+1)}{2}}} \tag{1.3}$$

where, c = velocity of light, $f_{\circ}$ = operating frequency, ε_r =dielectric constant of the substrate.

- Calculation of the effective dielectric constant (ε_{reff}) : This is calculated using the following equation;

$$\varepsilon_{reff} = \frac{\varepsilon_r+1}{2} + \frac{\varepsilon_r-1}{2}[1 + 12\frac{h}{W}]^{-\frac{1}{2}} \tag{1.4}$$

where, h = height of the patch in mm, W =is the width of the patch in mm.

- Calculation of the effective length of the patch (L_{eff}): The effective patch length is calculated using following equation;

$$l_{eff} = \frac{c}{2f_{\circ}\sqrt{\varepsilon_{eff}}} \tag{1.5}$$

- Calculation of the length extension (ΔL): The length extension is calculated using the following equation;

$$\Delta L = 0.412h\left[\frac{(\varepsilon_{reff}+0.3)\left(\frac{W}{h}+0.264\right)}{(\varepsilon_{reff}-0.258)\left(\frac{W}{h}+0.8\right)}\right] \tag{1.6}$$

where, ΔL = patch length extension in mm, h = patch height in mm and W =patch width in mm.

- Calculation of the actual length of the patch: the actual length of the patch antenna is calculated using the following equation;

$$L = L_{eff} - 2\Delta L \tag{1.7}$$

1.4 FEEDING TECHNIQUES

Various types of feeding techniques are available to feed microstrip antenna. Each of them has their own merits or demerits. A number of factors are used to choose which type of feeding is suitable for the designed antenna. The main consideration is effectual power transfer from feed line to the antenna radiating element that is proper matching between the feed and antenna. Various techniques like impedance transformer, stubs are used for impedance matching. Feed structure should like that these matching structure could be fabricated with radiating element easily. Spurious feed radiation

and surface wave losses are also the major factors which depend on the feeding methods which affects the antenna characteristics. Surface waves decreases the efficiency of antenna and spurious feed radiation results in undesired radiation which will give rise to side lobe level and also increases level of cross polarization. Another main feature is that feed network should be well-suited to make an array, feeding methods can be divided in two categories one is contacting feeds and other one is non contacting feeds or electromagnetic coupled feed. In contacting feeds the feed line is directly connected to radiating element. The main drawback of contacting feeds are that it shows inherent asymmetry which produces the higher order modes that leads to increase in cross polarization level. To minimize these non- contacting feeds are used. Microstrip line feed and coaxial probe feeding are two mainly used direct contact feedings and aperture coupled and proximity coupling are two non-contacting couplings which are described in brief in the next subsections. [2]

1.4.1 Microstrip line feeding

In this type of feeding the radiating patch is directly fed by the microstrip feed line has a narrow width as compare to patch. It is the simple and mostly used feeding method. Because microstrip line can be treated as extended part of radiating patch and fabricated on the same substrate on the board. This feeding simple to fabricate and it's easy to implement impedance matching techniques with this type of feed. But this feed also has some drawbacks, it suffers from spurious feed radiation and surface wave losses, it also supports a low bandwidth. Figure 1.4 shows a stripline fed MSA.

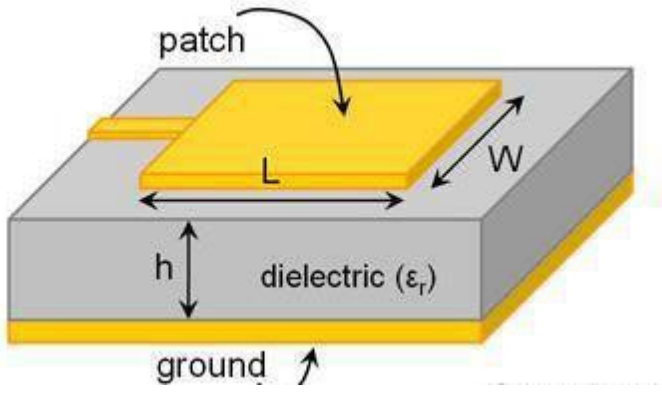

Figure 1.4 Microstrip Patch Antenna [2]

1.4.2 Coaxial probe feed

It is one of the widely used feeding for microstrip antenna. In this type of feeding core of coaxial cable is directly connected to the patch using the soldering and the outer cable are connected to the ground. Core conductor is inserted in the substrate via a hole. The main advantage of this feeding is that we can directly feed or connect the inner conductor to the feed point where the input impedance is equal to the characteristic impedance of the feed line. Figure 1.5 shows a coaxial fed MSA. [2]

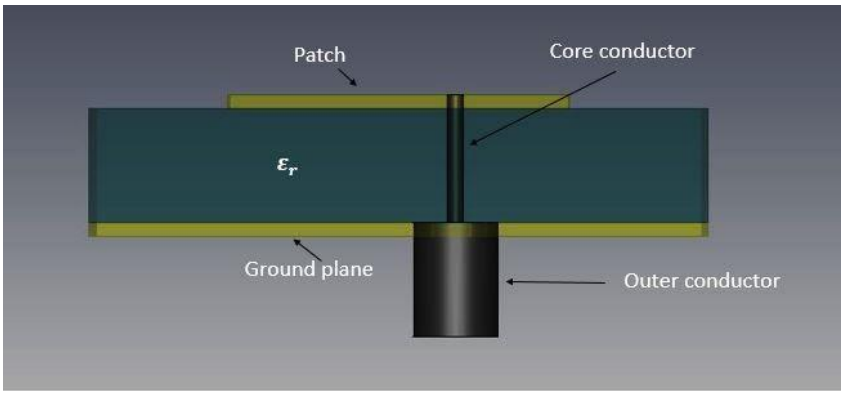

Figure 1.5 Coaxial Probe fed antenna [2]

1.4.3 Proximity coupled feed

Two types of dielectric substrates are used in this type of feeding. Microstrip line is not directly connected to patch and left open ended and is sandwiched between the substrates. Energy from feed line is coupled electromagnetically to the radiating patch. The microstrip line can be extended as stub to increase the bandwidth. Substrates dielectric constants play a lead role and selected to increase the bandwidth and decrease the spurious feed radiations from the feed line. Thick Material with low dielectric constant is selected for Upper substrates because lower the dielectric constant, more the fringing field and more the radiations from patch and thin substrate with high dielectric constant is selected for the lower substrate. This type of feeding has largest bandwidth as compared to others. It is easy to model and has low spurious feed radiation however its fabrication is more difficult because the exact alignment of feedline is required. The length of the extended stub and width to line ratio of patch can be optimized to control the antenna characteristics. Figure 1.6 shows a proximity fed MSA. [2]

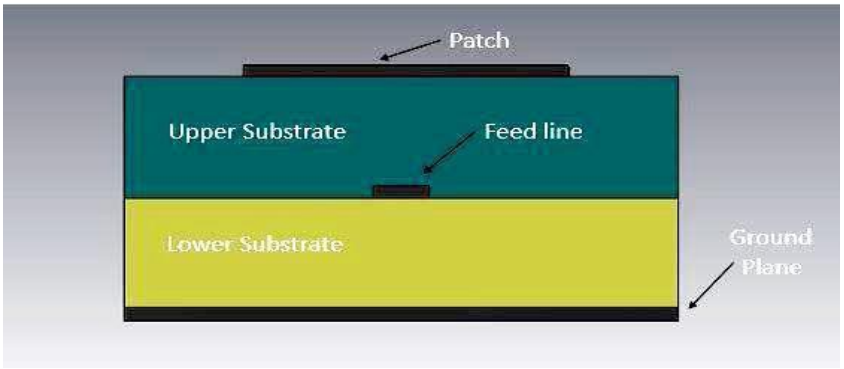

Figure 1.6 Proximity Coupled Antenna [2]

1.4.4 Aperture coupled feed

Structural view of this type of feeding is shown in Figure 1.7. As shown, this feeding also uses two types of substrates, ground plane is placed between them and microstrip line is used generally to feed which is placed below the lower substrate. As name suggests in aperture coupling feeding the energy is electromagnetically coupled to the patch through an aperture or slot made in the ground plane. Different types of aperture shapes are used generally rectangular and circular shapes are widely used. Cross shaped and annular ring shape slots are used for exciting the circular polarization. The parameters of slots are used to improve the antenna characteristics. As in proximity coupled feeding, substrates dielectric constant is selected to get better radiation and bandwidth. Thick substrate with low dielectric constant is used for the upper substrate to get the good radiation and bandwidth. While thin and high dielectric constant material is used for the upper substrate to for efficient transfer of energy from feedline to patch. To get the maximum coupling between feed structures, the patch slot should be located at the place where maximum magnetic field is present. [8]

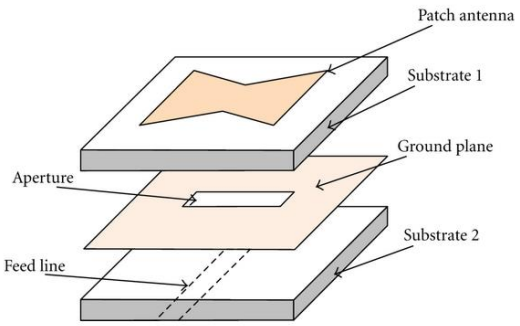

Figure 1.7 Aperture Coupling [2]

The area of slot is kept small to minimize the radiation below the ground plane. This type of feeding has better polarization purity, low spurious feed radiation and large bandwidth as compared to microstrip and coaxial probe feeding.

Table 1.1 Comparison of Various Feeding Techniques

Characteristics	**Micro-strip feed line**	**Coaxial feed**	**Proximity coupling**	**Aperture coupling**
Feed radation	More	More	Minimum	Less
Reliability	Better	Poor due to soldering	Good	Good
Bandwidth	2-5%	2-5%	21%	13%
Impedance matching	Easy	Easy	Easy	Easy

From the table 1.1, it can be concluded that aperture coupling is more reliable and can give good impedance matching. In contrast with microstrip feed line and coaxial feed line, the bandwidth offered by aperture coupling is more. For these reasons aperture coupling is used for all the antennas designed in the current research work presented in this thesis.

Since multiband antennas are required that can work at multiple wireless applications. Fractal engineering, a field was introduced. Next section deals with fractals in detail.

1.5 FRACTALS

Fractals is a term which is taken from a Latin word 'fractus' which means broken and it was first introduced to the world by B.B. Mandelbrot in 1977 [4]. Fractals are the structures which appear same at every scale that is why they are called self-similar objects. Fractals are found in nature and mathematicians were researching on it from a long period of time. Antennas which are made using the concept of fractals possess distinctive properties which has made them very popular among wireless communication applications [9].

Mandelbrot was the one who studied the relationship between fractals and natural object. Figure 1.8(a)-1.8(b) shows that many natural objects have been made successfully using fractals i.e. clouds, coastlines, tress, thunderbolt, snowflakes and mountain ranges. It is believed that human heart beat also follows fractal patterns. [10]

Figure 1.8(a) Snowflake [10]

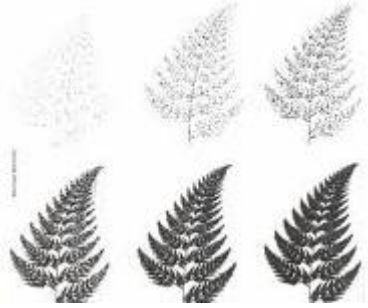

Figure 1.8(b) Tree pattern [10]

1.5.1 Fractal Antennas

The property of self-similarity in fractals can be used with MSAs to provide a new field of antenna design called Fractal antenna. Fractal antennas are self-similar structures and an iterative method is used to generate them. While designing these antennas the basic structure is scaled down in such a manner that the whole structure seems similar irrespective of the scale factor used. Multiband behavior of these antennas is the most unique and useful feature. The self-similarity at different scales leads to the surface current distribution which is also scalable at different operating bands which leads to multiband and log periodic behavior [11].

Due to increase in the path for threading current, the resonant frequency is lowered. The space-filling property of these antennas helps to minimize the size; such antennas may also be of infinite length and

can be packed in a finite volume. These two properties lead to small size of the antenna which will further be useful for size miniaturization of the modern devices and is very useful for wireless communication applications. [10]

1.5.2 Properties of Microstrip Fractal Antennas

The following table throws some light on some unique properties of the fractal antennas which have made them immensely popular.

- Fractals are self-similar structures. They are created by using copies of it but at different scales. The entire geometry is similar to the initiator and is easy to design.
- Fractal antennas have the property of space-filling. This property leads to the packing of more and more antennas in small volumes i.e. Hilbert Curve.
- Fractal antennas are designed using an iterative process. These antennas show multiband behavior corresponding to each iteration. Thus single antenna can radiate at more than one frequency.
- These antennas help in size miniaturization. These antennas resonate at lower frequencies with smaller physical size as compared to the ordinary antennas.
- These antennas are low profile, easy to model and fabricate and their cost of fabrication is also very less. It's just etching of copper over some dielectric substrate.
- These antennas are robust. They show much prevention against heat or mechanical strain.
- These antennas lead to packing of more energy in smaller volume which results in high quality factor.
- These antennas have sharp edges and discontinuities which help to increase the electrical length of the antenna and make it radiate efficiently
- These antennas are easy to feed and provide much flexibility to design and fabricate [11].

1.5.3 Types of Fractals

Mainly fractals are divided into two categories i.e. deterministic and random. Deterministic fractals are those which are generated using much iteration at different scale factors repeated copies using recursive algorithms. Random fractals make it possible to simulate natural phenomena because they show certain degree of randomness. Algorithms and mathematical functions can be found or developed for both [10].

A few fractals geometries are mentioned in the next subsections:

1.5.3.1 Sierpinski Fractal Antennas

These are the most popular geometries amongst all the fractals. These include Sierpinski Gasket, Carpet, Hexagon and Pentagon. Sierpinski Gasket antenna is the most popular geometry. Figure 1.9 shows the various design steps of the design procedure of the Gasket. An equilateral triangle is taken

as the generator in the zero iteration. [10] In the next iteration another triangle scaled down by a factor of two is subtracted from the generator such that vertices of the smaller triangle coincident with the mid points of the generator. This process can be repeated to a lot of iterations [10].

Figure 1.9 Design steps of the Sierpinski Gasket Fractal antenna [12]

These antennas show the multiband behavior and log periodic spacing between the resonant frequencies. Many other variations such that making a perturbed geometry and varying the flare angle are done and important conclusions were drawn from the results.

Another important Sierpinski geometry is Carpet which is very important in case size reduction is required. Carpet geometry can either be a square or rectangle. As shown in figure 1.10, to create the square carpet antenna initiator square is reduced by some scale factor and is cut from the center of the bigger square and in the next iteration the remaining area is divided into nine equal squares and in the next iteration same steps are repeated [10].

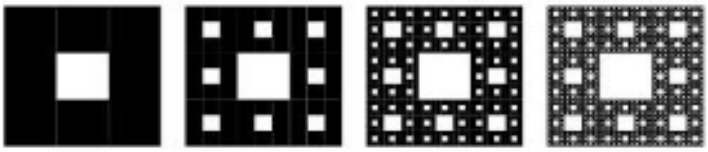

Figure1.10 Design steps of the sierpinski carpet antenna [10]

1.5.3.2 Koch Snowflake

In Koch snowflake an equilateral triangle is taken as the generator as shown in figure 1.11, the side of the triangle is divided into three equal segments and the central segment is removed and two segments are added to make an equilateral triangle. If this process is repeated several times the periphery of the island becomes infinite bounded in small space and the current travels longer distances to resonate at lower frequencies and also high quality factor [2].

Figure1.11 Design steps of the koch snowflake antenna [13]

Koch curve is popular due to its small size, wide bandwidth and directive properties due to higher modes propagation. If the iterative process explained above is applied for several times, the Koch Island becomes an antenna with infinite boundary resulting in the packing of more antenna length into a limited area and antenna with smaller size is obtained with resonance at lower frequencies also.

1.5.3.3 Hexagonal Sierpinski Fractal

Hex flake or Hexagonal Sierpinski has become so popular because of its multiband and wideband properties. In the design of Hexagonal Sierpinski antenna the original hexagon it replaced by seven hexagons whose side length is reduced by a factor of three. This antenna shows the multiband behaviour and log periodic behavior with the scale factor of three while the Sierpinski Gasket shows the same with the scale factor of two [2]. These antennas are useful where larger gap is required between the operating bands. The design steps for the hexagonal Sierpinski are shown in the figure 1.12

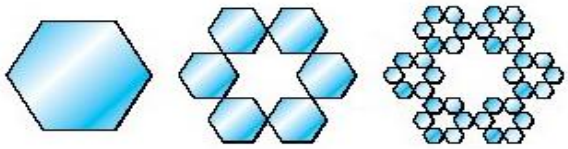

Figure 1.12 Design steps of the hexagonal fractal antenna [14]

Based upon the advantages mentioned in the above sections, an extensive literature survey was carried out in the field of aperture coupled fractal microstip antennas for wireless applications. Since a better SNR is demanded at the Rx side and MIMO antenna arrays are able to provide it successfully, some literature survey was carried out for MIMO microstip antennas. Many wireless applications require a selective frequency behavior, in terms of pass band and stop band so as to reduce interference from the nearby bands, therefore FSS (Frequency selective surface) were also studied and this literature survey is mentioned in chapter 2 in detail. A few research gaps were outlined and these are mentioned in the next subsection.

1.6 RESEARCH GAP

An extensive literature survey was carried out in chapter 2 that deals with the design and development of different types of fractal antennas for UWB applications, use of these fractal antennas for array

design and their utilization in MIMO systems. A few research gaps that were identified from the literature survey are mentioned below

- Not much work is available in the literature for using fractals in ground structure.
- Using aperture coupled feeding with fractal microstip antennas, is also an open area of research.
- Fractal antenna show multiband properties, using defected ground structures with the antennas in order to get an UWB behavior also an open area of research.
- Fractals can be used to make the antenna much smaller in size i.e. Nano size.
- A very less work is available in the literature on the use of fractal antenna arrays for MIMO applications.
- FSS (frequency selective surface) is new field where research can be done to design microwave filters and FSS based antennas.
- FSS can replace the normal microwave filters as they are more convenient as compared to others.

On the basis of the literature review and the research gaps found out; following objectives were defined for the current research work.

1.7 THESIS OBJECTIVES

Based upon the literature survey carried out and the research gaps highlighted in the literature survey following objectives were defined for the research work presented in this thesis:

- To design and simulate a conventional aperture coupled antenna at 2.4GHz and optimize its design for an improved bandwidth.
- To design and simulate a Sierpinski gasket fractal antenna for WLAN and STM applications and to extend this design to a MIMO system with two antennas at the Tx/Rx side.
- To design and simulate hexagonal fractal antenna for WLAN and X-band application & to extend the design to a MIMO system with two antennas at Tx/Rx side.
- To design and simulate a FSS based antenna for WLAN and X band applications.
- Fabrication & testing of a sierpinski gasket MIMO antenna array and a FSS based antenna.

The mentioned research objectives are achieved by carrying out the antenna design process using 3D EM tool CST MWS V'2016 software. Antenna arrays were designed for the desired results. The fabrication of these antenna arrays was done using photolithography process & their testing was done using VNA (E5063A) and (E5071C) for measurement of S parameter results.

The next subsection presents the thesis organization to carry out the mentioned research work.

1.8 THESIS ORGANIZATION

The thesis is divided into following chapters.

Chapter 1: Presents the introduction of MIMO systems, fractal antennas and MSA & use of fractal MSA in the current MIMO systems. Thesis objectives are also mentioned in this chapter.

Chapter 2: Presents the literature survey on patch antennas, fractal antennas, fractal with DGS and FSS

Chapter 3: Presents the conventional rectangular patch antenna and a Sierpinski gasket fractal antenna with single feed and this is then converted to a 2x2 MIMO antenna array.

Chapter 4: Presents a hexagonal patch antenna with DGS which is then converted to a 2x2 MIMO antenna array

Chapter 5: Presents a FSS (frequency selective surface) based antenna for WLAN, X-band applications.

Chapter 6: Presents the fabrication and testing of the antennas optimized in chapter 3 and 4. The antenna tested are a triangular sierpinski gasket array and triangular sierpinski FSS based antenna. The simulated and measured results are compared to see antennas applicability to practical scenario.

Chapter 7: Presents the Conclusions of the research work and its future scope

CHAPTER 2

LITERATURE SURVEY

2.1 INTRODUCTION

This chapter reviews the available literature on fractals microstrip antennas for multiband and ultrawide band applications. The use of defected ground structure for enhancing the bandwidth of operation is studied. The available MSA arrays are also studied for MIMO applications. A study of frequency selective surfaces is done and their uses in designing arrays for MIMO applications are also studied.

2.2 LITERATURE REVIEW

It presents the literature review on patch antennas, fractals, fractals with DGS and FSS (frequency selective surface).

2.2.1 Patch antennas

Kaur S. *et.al.* **[15]** Presented a staircase shaped patch and a flowery shaped ground shaped by which ultra-wideband was achieved. Different materials were also used for substrate and different shape of the patch to check the performance of the antenna.

Kaur A. *et.al*. [**16]** Presented a stacked patch sierpinski triangle shaped fractal antenna. Stacking was used to excite two resonant frequencies and by combining them an ultra-wideband was achieved. Defected ground was also used to improve the results. It was covering ultra-wide band and wireless local area network (WLAN).

Samsuzzaman M. *et.al.* **[17**] Presented an antenna of dimension $23 \times 21\ mm^2$ which covered the bandwidth 10.1 GHz (2.90-12GHz) and had a constant gain, stable radiation pattern and high efficiency. It could be seen that across the bandwidth it has radiation efficiency greater than85% and maximum of 98%.

Abdulhasan R. *et.al*. **[18]** Presented a compact size antenna that had U and J shaped slots in the patch for rejection of WiMAX and WLAN. It had a good performance over the entire frequency band(3.1GHz to 10.6GHz) except Wi-MAX(3.15-3.7GHz) and WLAN(5.15-5.85) GHz notched frequency band.

Khan M. *et.al.* **[19]** Presented an antenna in UWB region with large bandwidth and steady gain. It had a simulated impedance bandwidth of 57.8% centered on 7.3GHz with peak gain of 6.8dB. Variation in arm angle V-slot showed the tradeoff between quality of VSWR and bandwidth.

Sethi W. *et.al.* **[20]** Presented an antenna of compact design having dimensions $30 \times 30 \times 6.9\ mm^3$.This antenna was proposed to work for UWB RFID applications but it had one limitation that it provided limited bandwidth and gain. It covered a frequency band of 6-8GHz. The utilization of H-shaped aperture-coupled technique assisted in increasing the bandwidth and achieved high isolation between two orthogonal inputs.

Sze J. *et.al.* **[21]** Presented an antenna having a compact size of $25 \times 15\ mm^2$ and had a bandwidth from 3.06-16.5GHz. To produce better impedance matching with VSWR ≤ 2 the single strip of CPW had to be protruded into the aperture to form stub. Embedding in the aperture an additional grounded rectangular patch could lead to a desired notched band within the UWB.

Gatea K. *et.al.* **[22]** presented an ultra- wideband compact size antenna with total size of $25.5 \times 16 \times 1.6\ mm^3$. The impedance bandwidth of the antenna was 3.675GHz to 19.218GHz (about 15.5GHz). Here they used parasitic circles on the ground plane to reduce the ripples in low frequency. By embedding notches with proper dimension and perfect position good impedance matching and improved bandwidth was obtained.

2.2.2 Fractal

Darimireddy N. *et. al.* **[23]** presented a hexagonal fractal in which triangular slots were cut in the radiator. The size of the antenna was 25x30x0.8 mm^3. The antenna covered a bandwidth of 23.2 GHz from 3 GHz to 25.2 GHz with the gain value varying from 3 to 9.8dBi. This antenna had many applications covering (3–25.2) GHz, which includes all of the IEEE standard wireless frequency bands 3–6 GHz, UWB range 3.1–10.6 GHz, X band 8–12 GHz, and Ku band 12–18 GHz.

Angueral J. *et. al.* **[24]** This antenna presented a mandlebrot fractal antenna which was mainly designed for hotspots ie the requirement of the antenna was to achieve a narrow beamwidth in the vertical plane and a wide beamwidth in the horizontal plane. The same directivity and very similar patterns were obtained for the first high-directive mode (11.4 dBi in the simulation, 11.5 dBi in the measurement) with a measured total efficiency of 75%. Due to its rectangular profile, a narrow beamwidth 37° (3 dB beamwidth) in one plane and 66° in the perpendicular place was achieved for the built antenna.

El-Khamy1 S. *et. al.* **[25]** This paper presented a new antenna array design which proposed to combine the multi-band features of thinned fractal antenna arrays with the adaptive beamforming

requirements. The ACO algorithm was utilised as a synthesis method for thinning fractal antenna array using the SLL as optimisation parameter, while the LMS algorithm was employed to estimate the required excitation weights of the fractal array elements assuming the desired signal and several undesired signals were received by the array at respective directions of arrival.

Wang F. *et. al.* **[26]** This paper presented a compact antenna with Minkowski fractal geometry. By applying the Minkowski fractal geometry in the patch and the ground plane the miniaturization was achieved. The antenna had a size of 28x28mm^2 and covered a bandwidth from 700 MHz to 4.71 GHz with the average peak gain of 3.93 dBi.

Gorai A. *et. al.* **[27]** This paper presented a hexagonal shape fractal with Koch fractal boundary for UWB applications. The size of the antenna was 18.5x39 mm^2 which covered a Bluetooth frequency band centered at 2.4 GHz and WLAN application with band rejection at 5.5 GHz.

Kumar Y. *et. al.* **[28]** This paper presented a Koch snowflake with frequency reconfigurable antenna. The size of the antenna was 40x80mm^2 and was a triple band antenna covering bandwidth from 34–4.52 GHz, 2.2–3.4 GHz and 1.45–4.1 GHz was achieved.

Eichler J. *et. al.* **[29]** This paper presented a dual-band fractal antenna using modal methods. The size of the antenna was 50x50mm^2 with center frequencies at 1.25GHz and 2.1 GHz with relative bandwidth of 4.18% and 11.4% respectively. It was found that modal radiation patterns could successfully predict antenna radiation properties such as polarization or main lobe direction. Motif dimensions were noticeably smaller than a rectangular patch in both bands.

Hwang K. *et. al.* **[30]** This paper presented a dual wideband half-sierpinski gasket fractal antenna having bandwidth from 1.5GHz to 2.67 GHz and 5.135 GHz to 5.828 GHz. The antenna covered applications of GPS, DCS1800, PCS1800, UMTS, IMT-2000, WiBro (Wireless Broadband Internet Service), Bluetooth, S-DMB (Satellite Digital Multimedia Broadcast) and WLAN bands.

Romeu J. *et. al.* **[31]** This paper presented a new set of fractal multiband antennas called the mod Sierpinski gasket fractal. These triangles were derived from the Pascal traingle and have log-periodic behavior. The size of the antenna was 800x800mm^2 and had a bandwidth of 12.8 GHz from 0.2 GHz to 13 GHz for mod-3 and mod-5 antennas.

Ghatak R. *et. al.* **[32]** This paper presented an iris loaded cross dipole slot antenna. It was seen that by tapering the junction of the cross slots could results in wide impedance matching. Impedance bandwidth better than 2 GHz (9.6 to 12 GHz) was observed with a second iteration cross dipole fractal shape cantred slot antenna. It had a peak gain around 7 dBi.

2.2.3 Fractal with DGS

Singhal S. *et. al.* **[33]** In this paper a hexagonal fractal antenna was presented with square shaped slots and having coplanar waveguide feeding because of its coplanar nature, less losses, ease of fabrication etc.. Circular radiators had better bandwidth performance as compared to other structures that was the reason the hexagonal geometry was used in this design. Fractals have the property of getting a broadband characteristics without increasing the size of the antenna. In this design after implementing the 1st iteration the lower and higher band frequencies were shifted to the lower frequency and after the 2nd iteration the two operating band were converted into a broadband having a bandwidth coverage from 3.5 to 37.25 GHz. This design had the advantage that it was covering a wider bandwidth of 33.75 GHz with smaller size as compared to other structures.

Tripathi S. *et. al.* **[34]** this paper presented a hexagonal fractal antenna in which the radiator was of the shape of Koch snowflake. Fractal geometry has the property of resonating at multiple frequency which can be converted into ultra-wideband by combining them. The antenna was covering an ultra-wideband (UWB) bandwidth which is very popular now days because of its high data rates, low spectral density etc. Here the ground structure was also a fractal geometry which increased the electrical path length which also helped in enhancing the bandwidth of the antenna. The proposed structure had a compact size of 31x28x1.6 mm^3.

Wei K. *et. al.* **[35]** presented a new technique to design single feed CP microstrip antenna using Fractal Defected Ground Structure (FDGS). The CP microstrip antenna with second and third iterative FDGS were fabricated and 10-dB return loss bandwidth and 3-dB AR bandwidth have been reported as 30 MHz and 6MHz respectively. While the gain across CP band was 1.7 and 2.2 dBi.

Singhal S. *et. al.* **[36]** reported CPW fed octagonal super wideband fractal antenna for SWB applications. The experimental results validated the simulated data which reveal that the designed antenna helped in enhancing the impedance bandwidth. The fourth iterative structure of octagonal slot-loaded octagonal radiator, a coplanar waveguide feedline, and a modified ground plane design helped in achieving the impedance bandwidth of 3.8 - 68 GHz (179%). The proposed antenna design promised the advantages of wide bandwidth and miniaturized size over other antennas.

Kuzu S. *et. al.* **[37]** designed and manufactured a novel antenna with fractal shape and Defected Ground Structure (DGS) using Apollonius circles resulting in multi band compatibility with nested structure. This antenna proved to be efficient for geostationary satellite communication with higher gains and compact size in comparison to other antennas previously reported for the same application.

Upadhyay D. *et. al.* **[38]** investigated a hexagonal shaped fractal monopole antenna with defected microstrip structure for UWB applications. Introduction of spiral DMS and DGS slot on microstrip

feed fractal antenna increased the bandwidth and radiation characteristics as well as resulted in higher gains. The simulated results showed a return loss of less than – 10 dB in the frequency range of 2.7 – 9.2 GHz. The design helped to use such antennas for medical imaging, collision system in cars, etc.

Nagpal A. *et. al.* **[39]** designed and simulated a multiband E-shaped fractal patch antenna with DGS and FR-4 epoxy as substrate using IE3D software. This design helped the antenna to resonate at four different bands (3.7 GHz, 6.7 GHz, 7.9 GHz and 8.7 GHz.) with improved bandwidth (120 MHz, 495 MHz, 225 MHz and 315 MHz), gain (3.83 dBi, 4.90 dBi, 1.55 dBi and 4.26 dBi) and return loss (-15.61 dB, -16.99 dB, -12.18dB and -20.70 dB) in all bands. The antenna could be used in applications like Wi-Fi, Radar, Bluetooth, etc.

Ismail K. *et. al.* **[40]** presented a Sierpinski Gasket Fractal antenna with DGS designed using Computer Simulation Technology software where RT Duroid/RO5880 as substrate. The ring shaped DGS improved the overall efficiency with increased gain and reduction in size. The design proposed was suitable for RFID applications.

Colín-Beltrán E. *et. al.* **[41]** reported a novel Circular Aperture Slot Antenna (CASA) and a common mode (CM) noise rejection filter based on three non-periodical DGS. Radiation patterns for different frequencies were obtained in E and H planes. On comparison between the system with filter and one without filter, measurements in transversal plane showed attenuation up to 13 dB for system with filter. 127% of fractional impedance bandwidth was obtained by the system. The antenna reported can be used for broad band of operation.

2.2.4 FSS (Frequency selective surface)

Bashiri M. *et. al.* **[42]** This paper presented a FSS (frequency selective surface) structure having a size of 10x10mm^2 which was very less as compared to other FSS structures. There was only one substrate layer containing conductive material on both sides. On one side there was a loop and on the other side there was another loop with two folded arms. It was operational in three bands 3.2-3.7, 4.1-6 and 8-12 GHz which covered the applications of WiMAX, WLAN and X-band. It exhibits stable frequency response in different angles of incidence for TE and TM polarization.

Chatterjee A. *et. al.* **[43]** This paper showed that if we incorporate different curvature of a conformal FSS then wide range of beamwidth could be obtained. The antenna contained metallic wires which were forming quarter wave monopoles connected to each other by another metallic wire. This antenna was giving a dual response.

Li H. *et. al.* **[44]** this paper presented a dual polarized MAFSS (multifunctional active frequency selective surface). FSS (frequency selective surface) is a periodic array of metal which works as a filter. The most advantageous feature of MAFSS are electromagnetic switching, frequency tuning and polarization selection into a single design. The proposed surface had a thin substrate layer sandwiched between two metallic layers. The dielectric material was made up of F_4BME.

Taghizadeh M. *et. al.* **[45]** This paper presented a FSS (frequency selective surface) which was composed of non-resonant elements and uses patch elements rather than use aperture element to achieve band-pass response. This FSS covered a larger bandwidth (from 6.58 GHz to 18.83 GHz) and was more stable as compared to the other FSS structures or MFSSs structures. It covered the applications of X and Ku bands.

Li J. *et. al.* **[46]** This paper presented a bandpass filter based on FSS (frequency selective surface). The surface contained an array of rectangular slots. The structure wa fabricated using laser technology. It covered a total bandwidth of 400 GHz with 1 THz as a center frequency and had applications in terahertz communication, imaging and sensing systems, for its excellent performance and easy fabrication.

Yang S. *et. al.* **[47]** This paper presented an Ultra-thin FSS (frequency selective surface) with dual passband at 8.2 GHz and 11.4 GHz which could be tuned independently. The single ended short resonator reduced the unit cell and the electromagnetic coupling also made the overall structure thin.

Hua B. *et. al.* **[48]** This paper proposed a FSS structure which was based on 2.5D MHRs could provide an ultrawide band stopband. The bandwidth coverage was from 1.97 GHz to 8.08 GHz. It provided good polarization-independent performance. The structure was fabricated and the measured results were almost same as were in simulated graphs.

Liu N. *et. al.* **[49]** this paper proposed a band-stop FSS (frequency selective surface). Transmission line model was used first to get an equivalent circuit model of the structure. The design consisted of two square loops arrays which were separated by a substrate. The fractional bandwidth provided by the structure is 88.9% with band-stop operating at 13.5 GHz.

Based upon the literature survey carried out in this chapter, a few research gaps were outlined, which are mentioned in chapter 1 (section 1.7). These research gaps were used to define the objectives of the research work carried out in this thesis mentioned in section 1.8. Next four chapters deal with each objective and the details of how each is carried out are also mentioned accordingly.

CHAPTER 3

DESIGN AND SIMULATION OF AN APERTURE COUPLED MSA AND IMPLEMENTATION OF APERTURE COUPLING TO A SIERPINSKI GASKET FRACTAL ANTENNA ARRAY FOR MIMO APPLICATIONS

This chapter presents the design of a conventional modified rectangular patch antenna for wireless local area network (WLAN) covering a band from (2.364-2.5034) GHz. This antenna is fed using aperture coupled feeding mechanism.

The same feeding method is then used to design a compact triangular Sierpinski gasket fractal ultra-wide band (UWB) for WLAN applications. The antenna covers a frequency band from 5.4859 GHz to 6.4902 GHz with bandwidth of 1.006 GHz suitable for IEEE 802.11, C-band and STM applications. This triangular Sierpinski gasket fractal antenna is extended to an array design with two triangular Sierpinski fractals with a $3 \times \frac{\lambda}{2}$ spacing between their centers. This array is then suitable for MIMO wireless applications.

3.1 THEORETICAL ANALYSIS

Aperture coupled feed is one of the best feeding techniques among all the techniques [16]. It has a ground structure sandwiched between two substrate layer, on the upper substrate there is a radiator and on the lower substrate there is a feed line. It is easy to implement and covers larger bandwidth. The antenna proposed here is a simple rectangular patch in which sides are sliced and the ground is also made defected to get a larger bandwidth. The antenna is designed on an FR4 substrate with $\varepsilon_r = 4.4$ and $h = 1.57mm$. By using equations 3.1-3.5, the dimensions of the patch and substrate can be calculated for a resonant frequency of 2.4 GHz.

$$w = \frac{c}{2f_\circ\sqrt{\frac{(\varepsilon_r+1)}{2}}} \tag{3.1}$$

$$\varepsilon_{eff} = \frac{\varepsilon_r+1}{2} + \frac{\varepsilon_r-1}{2}\left[1 + 12\frac{h}{W}\right]^{-\frac{1}{2}} \tag{3.2}$$

$$l_{eff} = \frac{c}{2f_\circ\sqrt{\varepsilon_{eff}}} \tag{3.3}$$

$$W = 6h + w \tag{3.4}$$

$$L = 6h + l \tag{3.5}$$

Where,

w= width of the patch, c=speed of light, $f_\circ$= resonant frequency, ε_r =dielectric constant, h=height of the substrate, ε_{eff}= effective dielectric constant, L_{eff}=effective length of the patch, W=width of the substrate, L= length of the substrate [2]

According to the above equations the dimensions of the patch, substrate and ground can be calculated. After analyzing aperture coupled feeding mechanism a triangular Sierpinski gasket fractal is designed using the same feeding.

Figure 3.1 shows the layered architecture of the designed conventional rectangular MPA with aperture coupled feed, the antenna shape is modified to get a wideband shown in Figure. 3.2(a). All design parameters are mentioned in table 3.1

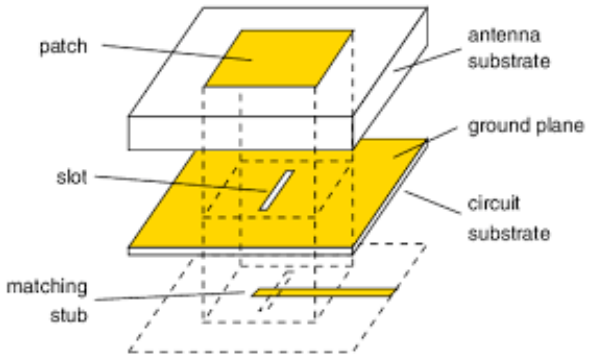

Figure 3.1 Designed conventional patch antenna with an aperture coupled feed

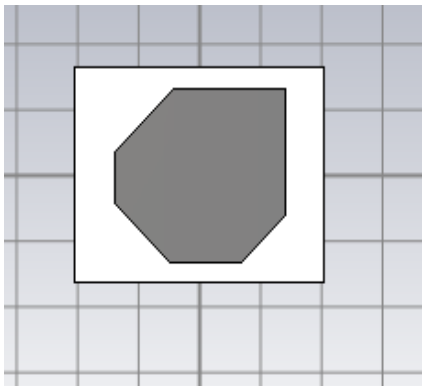

Figure 3.2(a) Top view of antenna

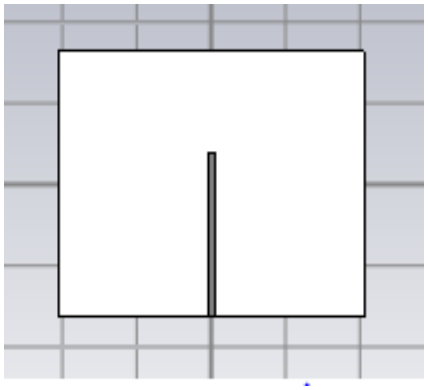

Figure 3.2(b) Back view of antenna

Table 3.1 Specified Antenna Parameters for antenna at 2.4 GHz

Parameters	**Value**
Resonant frequency	2.4ghz
Patch substrate material	Fr 4
Patch substrate thickness	1.57mm
Dielectric constant of the material used	4.4
Thickness of PEC material	0.035mm

Parameters	Value
Length of patch	28.036mm
Breath of patch	26.404mm
Length of substrate	41.036mm
Breath of substrate	32.624mm

3.1.1 Antenna Simulation Results

Simulation results in CST MWS V'16 such as impedance bandwidth, gain, current distribution are mentioned in next subsections.

3.1.1.1 Return loss and antenna bandwidth

Figure. 3.3 shows graph between return losses versus frequency for the proposed antenna. It covers a frequency range between (2.364-2.5034) GHz with a bandwidth of 139.4 MHz with return loss value of -34dB at a resonant frequency of 2.4GHz. This frequency band covers WLAN applications successfully.

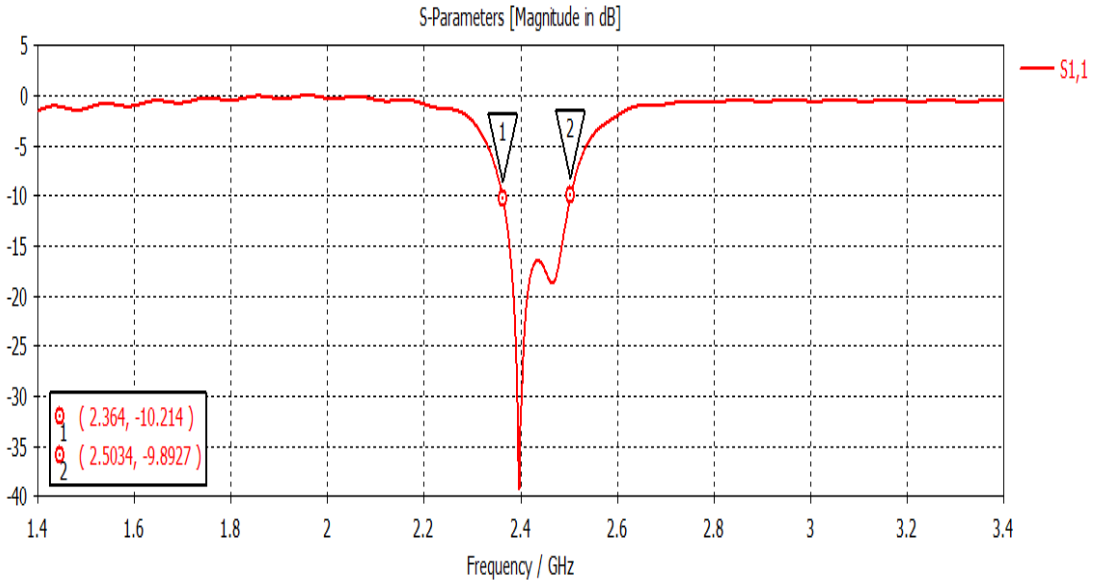

Figure 3.3 Return Loss S_{11} (dB) v/s Frequency plot of antenna at 2.4 GHz

3.1.1.2 Current Distribution

The Figure. 3.4 shows the current distribution of the radiator at 2.4GHz. The antenna parts that show maximum current distribution at 2.4 GHz are responsible for exciting that frequency of operation. Current distribution helps in antenna optimization process.

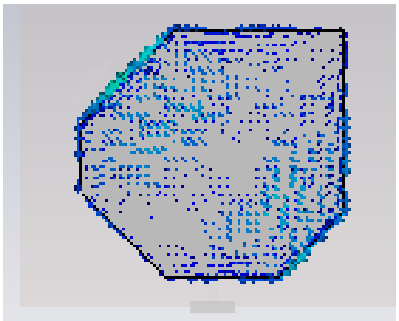

Figure 3.4 Current distribution at 2.4 GHz

3.1.1.3 Antenna gain and radiation pattern

Figure. 3.5 shows the radiation pattern plot of the simulated antenna designed at 2.4 GHz. Gain is a measure of the amount input power converted to output power for a given direction of antenna radiation. The proposed antenna has gain of 4.360 dBi at the resonant frequency of 2.4 GHz.

Polar plot convey the information about the antenna directivity, the major and minor lobes and half power beamwidth. It can be seen in the figure 3.5 the 3dB angular width is 122.9 along 1 degree of antenna's elevation view.

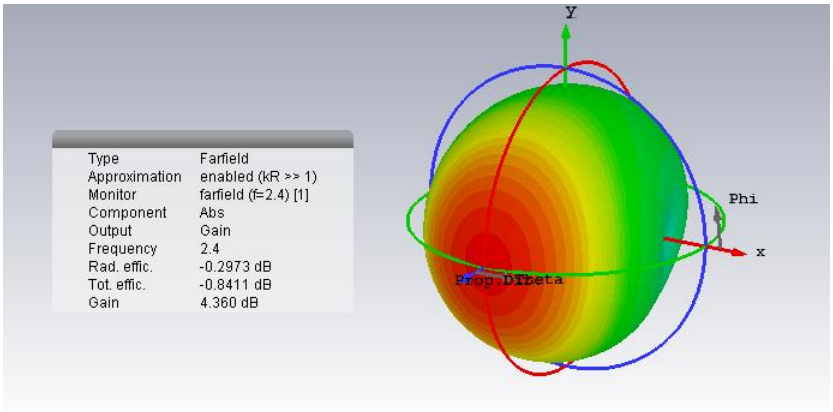

Figure 3.5 3D Radiation Pattern of the Gain of the antenna

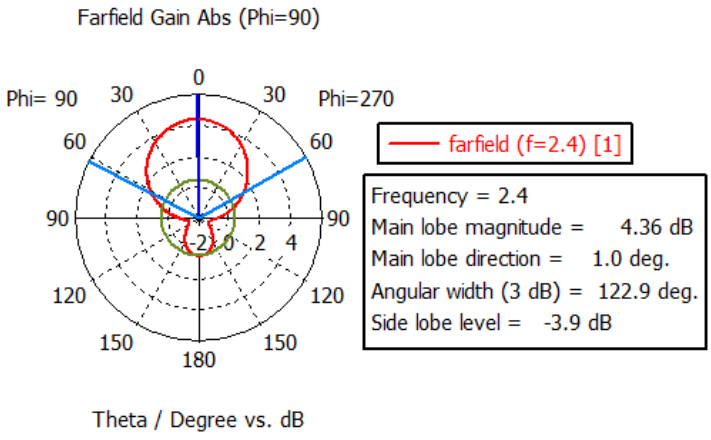

Figure 3.6 Polar plot of the proposed antenna

3.2 DESIGN OF A TRIANGULAR SIERPINSKI GASKET FRACTAL ANTENNA WITH APERTURE COUPLING APPLICATIONS

A compact triangular Sierpinski gasket fractal ultra-wide band (UWB) for WLAN application is presented here. The overall area of the antenna size is 115x37x3.245 mm^3. The antenna has a defected ground structure with a cross shaped slot. Three slots are added in the ground layer to this slot in order to get the desired UWB operation from the antenna. The antenna covers a frequency band from 5.4859 GHz to 6.4902 GHz with bandwidth of 1.006 GHz suitable for IEEE 802.11, C-band and STM applications.

This triangular Sierpinski gasket fractal antenna is extended to an array design with two triangular Sierpinski fractals with a $3 * \frac{\lambda}{2}$ spacing between their centers. This array is then suitable for MIMO wireless applications. MIMO systems offer better SNR and thus can lead to a better output even with a low transmitted power.

3.2.1 Theoretical Analysis of the Triangular Sierpinski Gasket Fractal Antenna

The sierpinski fractal antenna is constructed by creating an equilateral triangle and then subdividing algorithmically into smaller equilateral triangle. [4] The equations used for the designed sierpinski fractal antenna are given below.

$$f_{m,n,1} = \frac{2c}{3ae_{ff}(\varepsilon_{reff})^{\frac{1}{2}}}(m^2 + mn + n^2)^{\frac{1}{2}} \tag{3.6}$$

$$a_{eff} = a + h(\varepsilon_r)^{-\frac{1}{2}} \tag{3.7}$$

$$\varepsilon_{eff} = \frac{1}{2}(\varepsilon_r + 1) + \frac{1}{4}(\varepsilon_r - 1)(1 + \frac{12h}{a})^{-\frac{1}{2}} \tag{3.8}$$

Where,

'a' is the length of the equilateral triangular patch,

h=thickness of the substrate,

ε_r= relative dielectric constant,

c= velocity of light and

$TM_{m,n}$ = resonant fundamental mode where m=0, n=1.

At the first stage single sierpinski gasket fractal antenna is designed, slots were cut in the ground one by one and its simulated S-parameter were measured to get the optimized structure. The antenna shows an ultra-wide band which is covered between 5.5133 to 6.5032 GHz. The triangular antenna is simulated upto three iterations. The front and back view of the design is shown in figure. 3.7 (a, b)

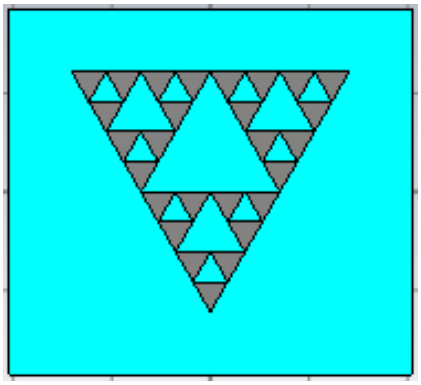

Figure 3.7(a) Front view of the antenna

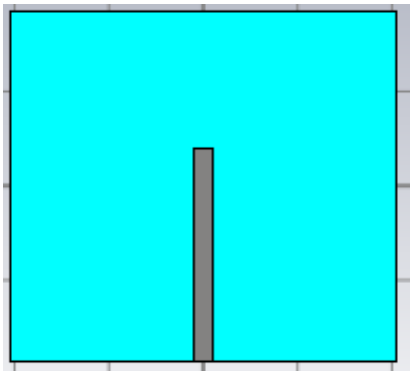

Figure 3.7(b) Back view of the antenna

3.2.2 Simulated results

This section covers the simulated results using CST MWS V'2016 of the antenna such as impedance bandwidth, radiation pattern, Gain and current distribution.

3.2.2.1 S_{11} parameter bandwidth

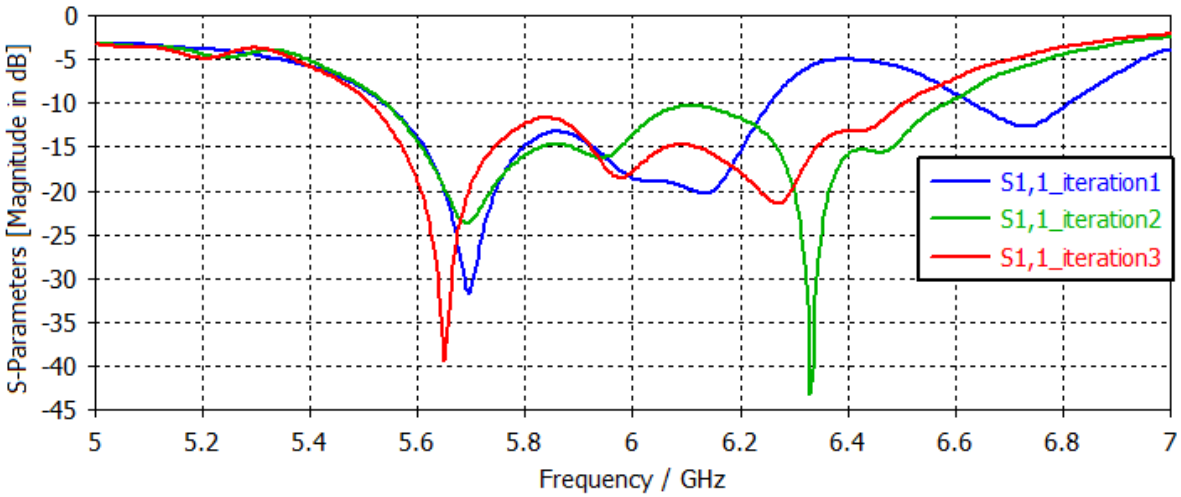

Figure 3.8 S-parameter of the proposed antenna

Figure. 3.8 shows the simulated S_{11} parameter plot of antenna versus frequency. The antenna was optimized upto three iterations. Figure 3.2 shows best results for the third iteration & the antenna is therefore optimized at this iteration.

3.2.2.2 Gain and radiation pattern

Figure 3.9 (a, b) show the radiation pattern of the proposed antenna at 5.7 GHz and 6.2 GHz respectively. The antenna show a gain of 5.85 dBi at 5.7 GHz and 3.47 dBi at 6.2 GHz which is considered as a good gain for short range applications.

Figure 3.10 (a, b) shows the polar plots at 5.7 GHz and 6.2 GHz. Polar plot indicate the direction of main lobe where the antenna is radiating more as compared to the other directions. At 5.7GHz the major lobe is directed along 76 degree and has a beamwidth of 82.9 degree. At 6.2 GHz the major lobe is directed along 182 degree and has a beamwidth of 42.8 degree.

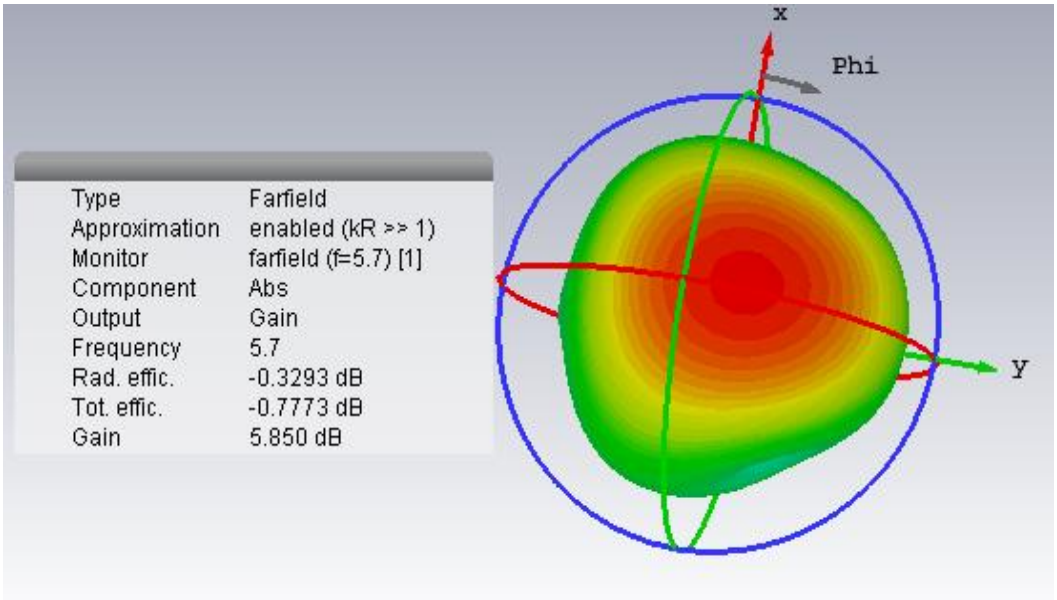

Figure 3.9 (a) Radiation pattern of the proposed antenna at 5.7 GHz

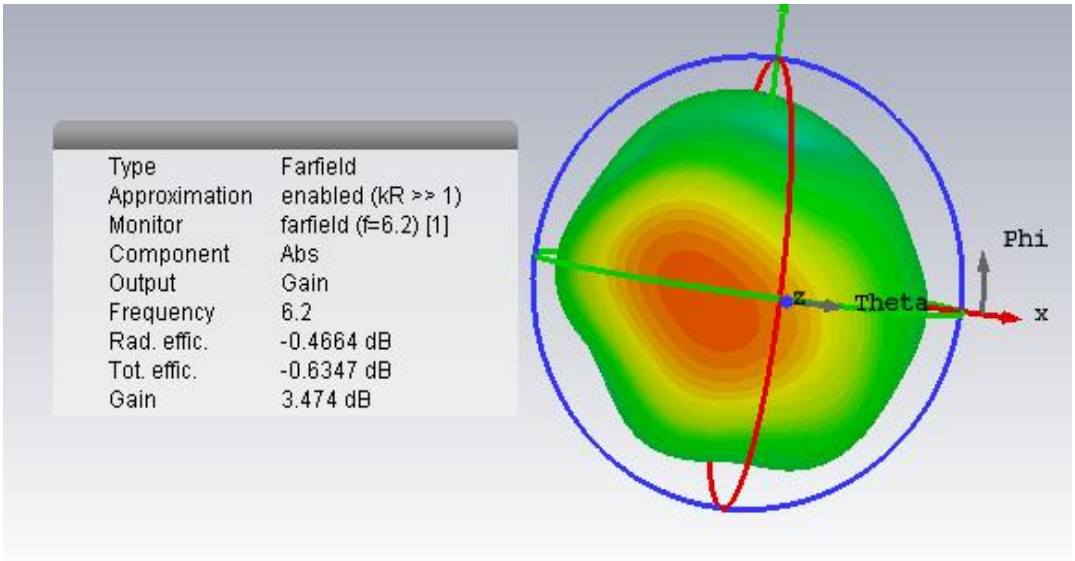

Figure 3.9 (b) Radiation pattern of the proposed antenna at 6.2 GHz

Figure 3.9 (a) and (b) show that the antenna has a radiation efficiency of 0.3292dB in the farfield and at an operating frequency of 5.7 GHz and a radiation efficiency of 0.4664Db at the operating frequency of 6.2 GHz .

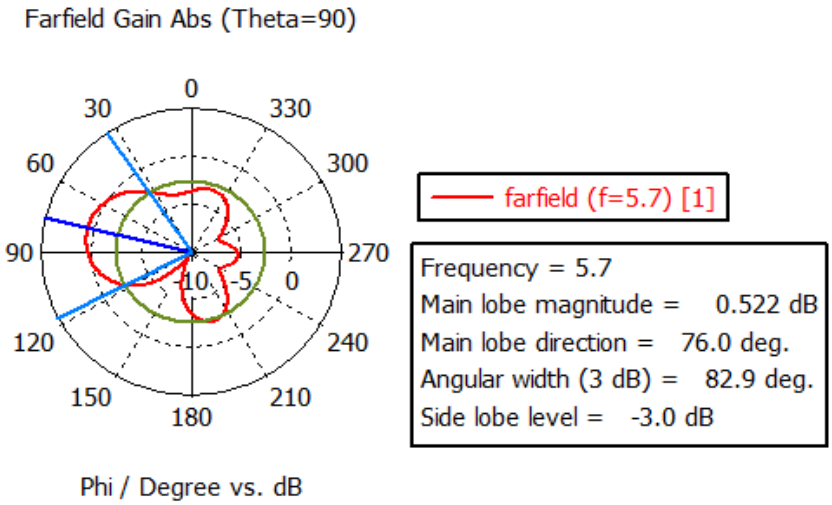

Figure 3.10 (a) Polar plot of the proposed antenna at 5.7 GHz

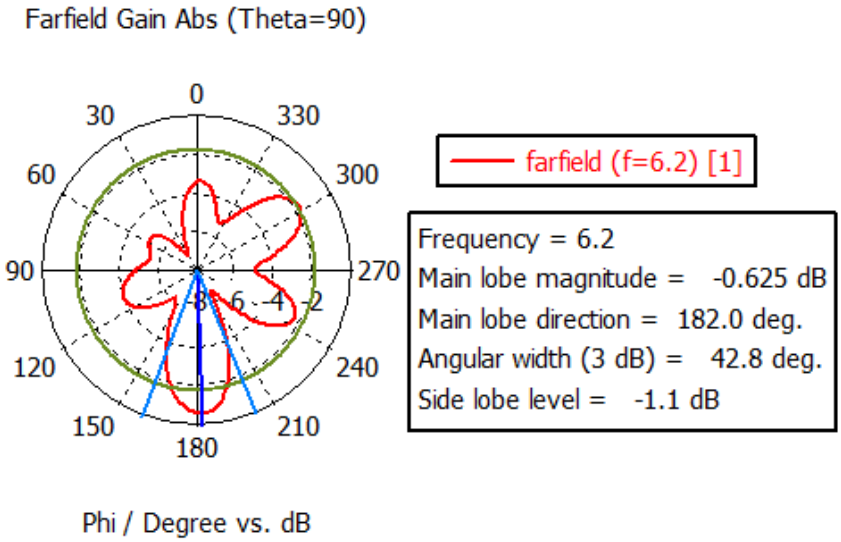

Figure 3.10 (b) Polar plot of the proposed antenna at 6.2 GHz

3.2.2.3 Current distribution

The Figure 3.11(a, b) shows the distribution of energy on the antenna patch surface at 5.7 GHz and 6.2 GHz, when the antenna is excited in the TE_{10} mode. Due to slots in the patch, current loops are formed to excite the required frequency bands. A peak current density of 114.9 A/m is available on the antenna patch at 5.7 GHz and 143.2 A/m at 6.2 GHz.

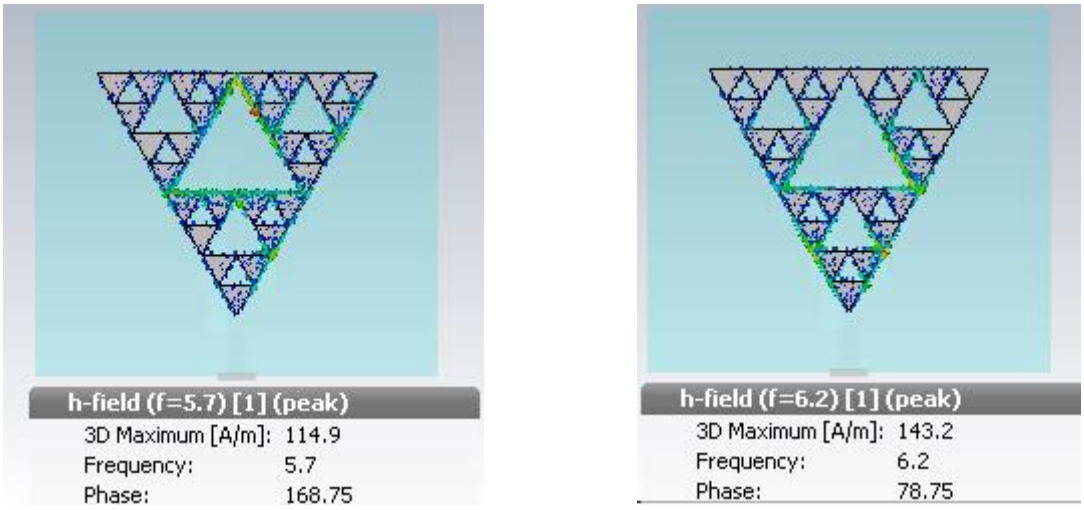

(a) (b)

Figure 3.11 (a, b) Shows the current distribution in the patch at 5.7 GHz and 6.2 GHz

3.3 SIERPINSKI GASKET TRIANGULAR ANTENNA ARRAY FOR MIMO APPLICATIONS

The proposed triangular Sierpinski gasket fractal antenna with a DGS is extended to an array design. Here two triangular antennas with aperture coupled feeding are designed with spacing between their centers as $3 * \frac{\lambda}{2}$. The array proposes a good bandwidth with low ECC & a high diversity gain for MIMO WLAN applications.

3.3.1 Theoretical analysis

The antenna designing is carried out using equations mentioned in section 3.1. The antenna array is designed on an FR4 substrate with $\varepsilon_r = 4.4$ &$h = 1.57\ mm$.

As discussed in section 3.2, the antenna is iterated upto three level of iterations & with an 'F' shaped DGS with distance between the patches$3 * \frac{\lambda}{2}$.

Figure. 3.12 shows the perspective view of a triangular Sierpinski gasket fractal antenna array with two radiators and an aperture coupled feeding.

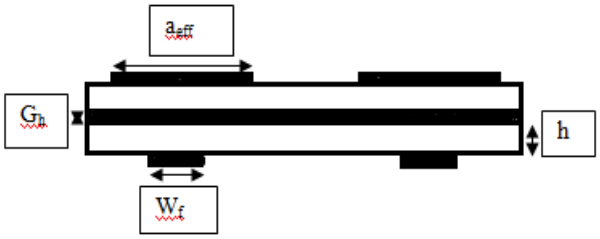

Figure 3.12 Front view of antenna

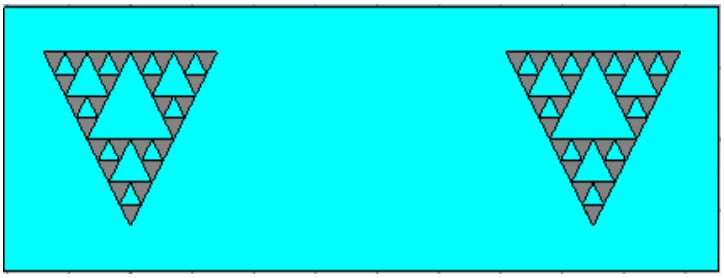

Figure 3.13(a) Top view of the antenna array

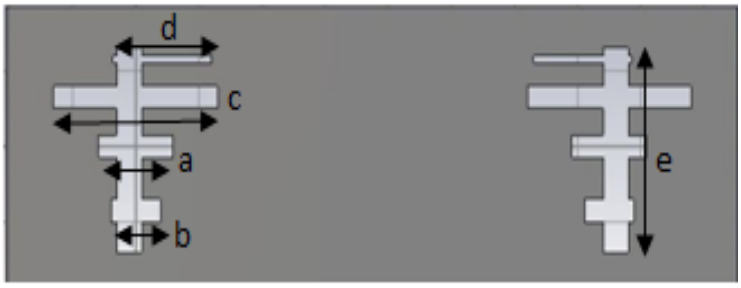

Figure 3.13(b) Top view of the antenna ground

Figure 3.13 (a, b) show the top view of antenna array and the defected ground structures respectively.

There are two radiating sierpinski fractal patches with 3nd degree of iteration above the substrate 2 which are kept at a distance of (3*λ/2) so that there radiation does not cancel each other's gain. The dimensions of the parameters used in the antenna are given below in the table.

Table 3.2 Dimensions of optimized parameters of the proposed antenna

Parameters	**Dimensions (mm)**	**Parameters**	**Dimensions (mm)**
a	11.8	h	1.57
b	7.84	W_f	2.1
c	26	G_h	0.035
d	15.6	a_{eff}	28.1691
e	27		

3.3.2 Simulated results

The antenna array simulation results in CST MWS V'16 are presented in next subsections

3.3.2.1 Antenna return loss and bandwidth

Figure. 3.14 shows the simulated result of the S-parameter for the designed MIMO antenna.

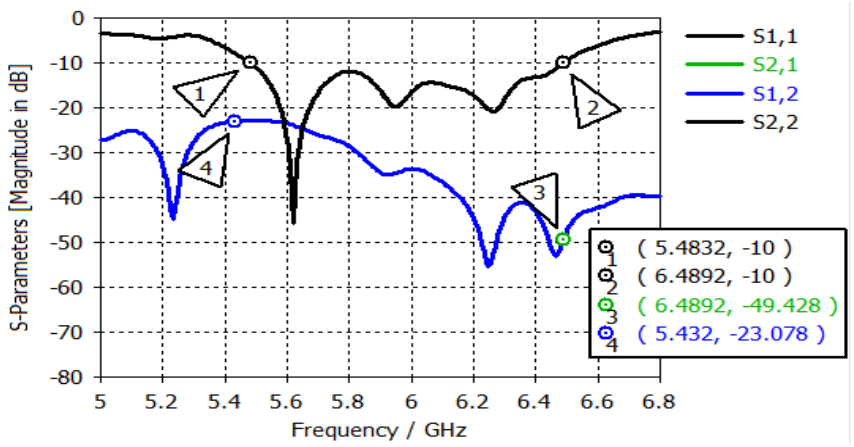

Figure 3.14 Simulated value of S-parameter

The antenna covers a bandwidth of 1.006 GHz from (5.4832-6.4892) GHz with S_{11}/S_{22} < 10dB and S_{12}/S_{21} <20dB. The transmission coefficient of the antennas in the array is quite low & allows the array to be good candidate for MIMO applications.

The three iterations help in achieving multi bands & DGS resonant at the same bands improves bandwidth by combining nearby bands to achieve UWB characteristics.

3.3.2.2 Current Distribution

The Figure. 3.15 shows the distribution of energy in the antenna at 6GHz when the antenna is excited in the TE_{10} mode. For coupling to be the maximum slots are cut in the ground which create multiple current loops and thus result in UWB of 1.006 GHz bandwidth from 5.4832 GHz to 6.4892 GHz.

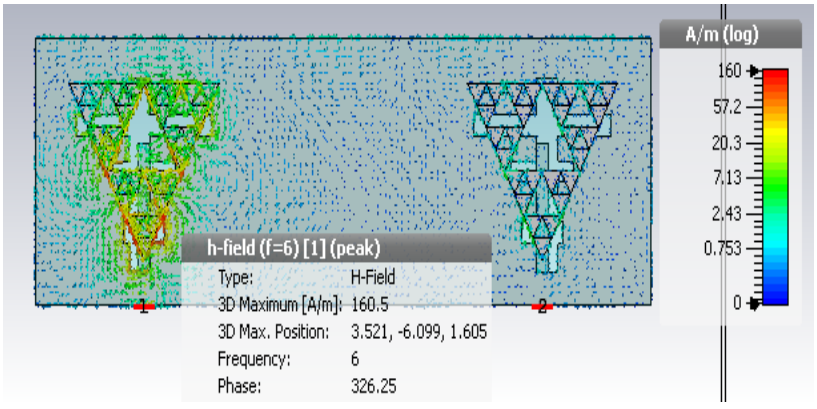

Figure 3.15 Current distribution at 6GHz

3.3.2.3 Radiation Pattern and Gain

Figure. 3.16 Depicts the broadband gain of the proposed antenna array. The simulated array shows average gain of 4.9dB (approx.) for the entire band and has a peak gain of 5.21dB. Figure. 3.11

Shows the radiation pattern of the proposed antenna at 5.7GHz the antenna array shows a radiation efficiency -0.371 dB at this frequency of operation.

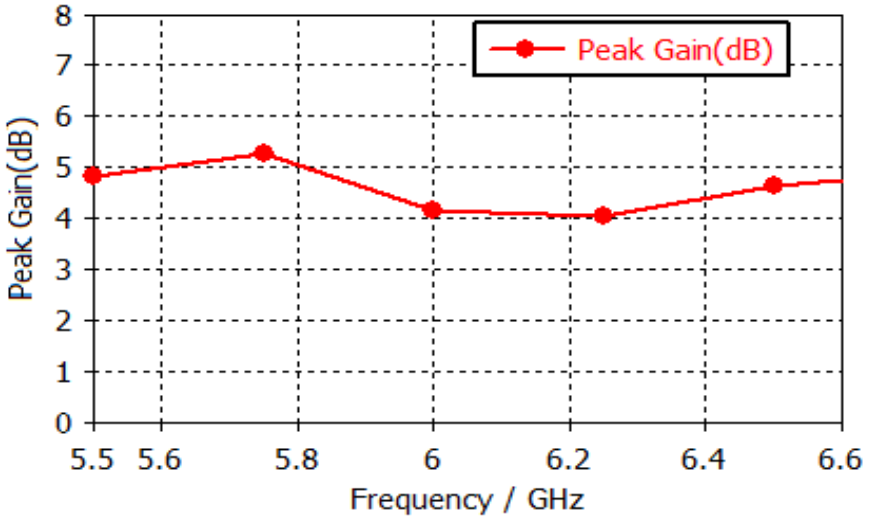

Figure 3.16 Broadband gain of the antenna.

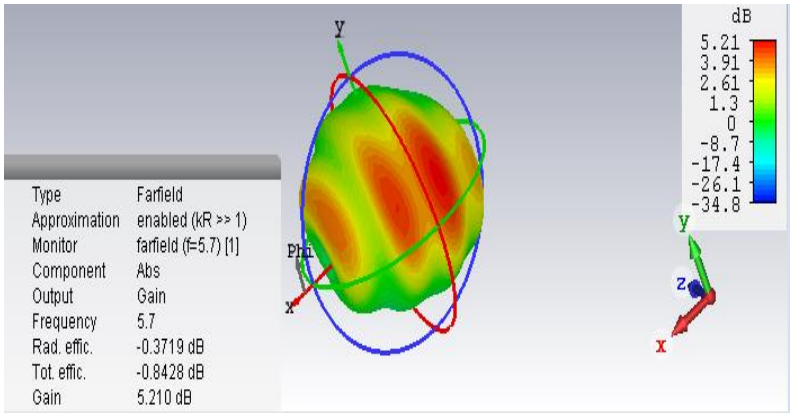

Figure 3.17(a) Antenna radiation pattern at 5.7GHz

Polar plot convey the information about the antenna directivity, the major and minor lobes and half power beamwidth. It can be seen in the figure 3.17(b), the 3dB angular width is 34.2° along 36° of antennas elevation plane of radiation.

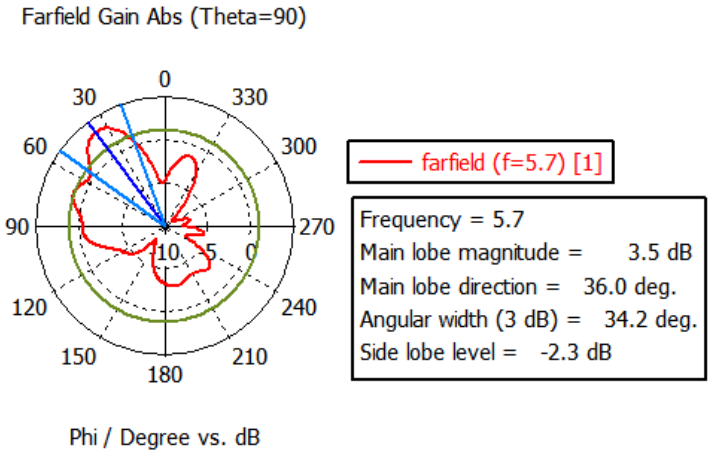

Figure 3.17(b) Polar plot of the proposed antenna at 5.7GHz

3.3.2.4 Envelope correlation coefficient

When MIMO antennas are considered envelope correlation coefficient (ECC) plays a major role as it indicates how correlated the antennas are in the array, i.e. how much interference the antenna are providing to each other while radiation. For a satisfactory performance low envelope correlation coefficient (ECC) is required. [7] The ECC can be calculated by using S-parameters by the following equation for a 2x2 antenna.

$$ECC = \frac{|S_{11}^{*}S_{22}+S_{21}^{*}S_{12}|^{2}}{(1-|S_{11}|^{2}-|S_{21}|^{2})(1-|S_{22}|^{2}-|S_{12}|^{2})} \tag{3.9}$$

The ideal value of the ECC is zero but practically value of the uncorrelated MIMO antenna should be ECC<0.5. The value of the ECC for the designed antennas in the array is ECC<0.002 shown in Figure 3.18 for the entire UWB which is very good as it close to zero.

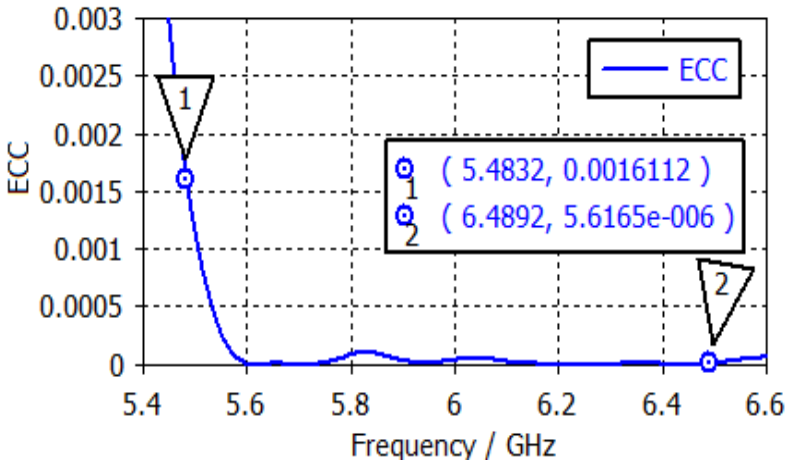

Figure 3.18 EEC of the proposed antenna

3.3.2.5 Diversity Gain

Diversity gain (DG) is another parameter which is taken care of MIMO antenna performance analysis is done and it is given by the equation.

$$DG = 10\sqrt{1-(ECC)^{2}} \tag{3.10}$$

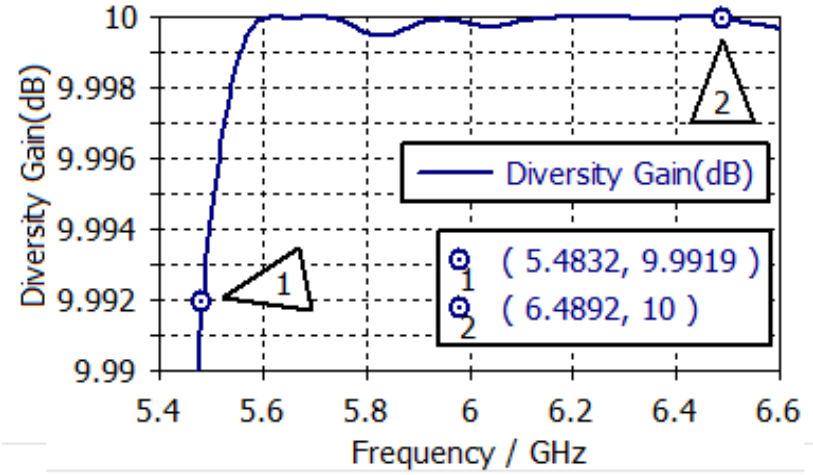

Figure 3.19 Diversity gain of the proposed antenna array

The ideal value of the diversity gain is 10 when the value of ECC is considered to be zero. Figure 3.19 shows the value of the ECC <0.002 so that the value of DG is greater than 9.99 for the entire band.

3.4 CONCLUSION

This chapter presented the design & simulation of a rectangular modified antenna with aperture coupled feeding for IEEE 802.11 applications. It covers a band from 2.364 GHz to 2.5034 GHz. Aperture coupled feeding is used to design a triangular Sierpinski gasket fractal antenna. This covers a band from 5.5133 GHz to 6.5032 GHz with bandwidth 0.989 GHz for IEEE 802.11, C-band and for STM band applications

A compact sierpinski gasket microstip antenna array for IEEE 802.11, C-band and for STM band applications is then presented with the same feeding mechanism. The proposed antenna shows an ultrawide band performance of 1.006 GHz from 5.4832 GHz to 6.4892 GHz, as a result making it suitable for WLAN band from 5.75-5.856 GHz, STM band from 6-6.17 GHz and C-band from 5.850-6.425 GHz. The antenna array shows an average gain of 4.14dB over entire band of operation that suits short range applications. A low correlation coefficient of ECC<0.002 allows the two antennas to be uncoupled when used for WLAN MIMO applications, thereby not providing interference to each other. The antenna array has a high diversity gain of 9.99dB which allows the antennas to give good output when used in a 2 X 2 configuration at even transmitted low power.

CHAPTER 4

DESIGN AND SIMULATION OF A MULTIBAND HEXAGONAL ANTENNA WITH DGS & ITS IMPLEMENTATION TO AN ANTENNA ARRAY FOR MIMO APPLICATIONS

A compact size dual band hexagonal antenna with DGS is presented in this chapter. The antenna resonates at two frequency bands namely 5.2 GHz and 9.2 GHz with a bandwidth of 241.2 MHz and 981.2 MHz resp. The antenna is designed with a DGS for WLAN and X-band applications. This antenna is extended to an array with two hexagonal patches and two feed networks on the substrate. The antenna array has very low value of ECC (< 0.0034) and mutual coupling is less than 18dB between the antennas of the array and hence the interference between the two antennas is very low. Additionally the array possesses a good diversity gain of 9.98dB. The chapter presents the antenna array simulation results in terms of impedance bandwidth, current distribution, correlation coefficient and broadband gain and thus presents its applicability to the current MIMO WLAN and X band scenario for a good data rate.

4.1 THEORETICAL ANALYSIS

The work starts with design of a hexagonal MSA on an FR4 substrate with $\varepsilon_r = 4.4$ &$h = 1.57\ mm$. The design is then extended to an array with two hexagonal antennas placed $\frac{\lambda}{2}$ apart with individual feed network for each.

The resonance frequency of hexagonal microstrip antenna can be designed using the equation

$$f_r = \frac{\chi_{mn} c}{2\pi a \sqrt{\varepsilon_r}} \tag{4.1}$$

Where f_r; resonance frequency X_{mn}=1.8411 for the dominant modeTM_{11}, c=velocity of light in free space, ε_r = relative permittivity of the substrate where as effective radius of circular microstip antenna is given by

$$a_e = a\left\{1 - \frac{2h}{\pi a \varepsilon_r}\left(ln\frac{\pi a}{2h} + 1.7726\right)\right\}^{1/2} \tag{4.2}$$

In the above expression, ‘a’ is the actual radius of the circular patch antenna, ‘h’ is height of the substrate and ε_r is relative permittivity of the substrate. This antenna comprises of a hexagonal fractal in which single iteration has been done with defected ground to get a fair amount of gain.

Hexagonal microstrip patch antenna is one of the various shapes capable for circular polarization. The design of hexagonal microstrip antenna can be done by using variation of static energy below hexagonal circular patch. The relationship between the equivalent areas of circular and hexagonal patches in given

$$\pi a_e^2 = \frac{3\sqrt{3}}{2} S^2 \quad (4.3)$$

Where, S is side of hexagonal patch and a_e is effective radius of circular patch [13]. Figures. 4.1 & 4.2 show the front & back view of the MSA with an aperture coupled feed.

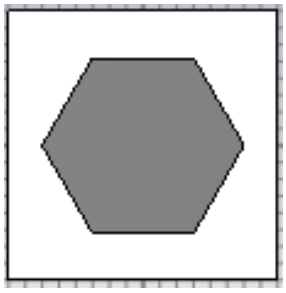

Figure 4.1 Front view of the antenna

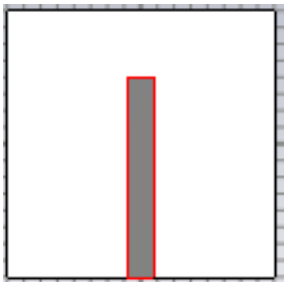

Figure 4.2 Back view of the antenna

4.2 Simulation results

Antenna was simulated using CST MWS V 2016 software. This section presents the simulation results in terms of S –parameter, gain, radiation pattern and current distribution.

4.2.1 Return loss

The antenna resonates at two band, one centered at 5.2 GHz with bandwidth of 241.1 MHz and another at 8 GHz with bandwidth 981.2 MHz.

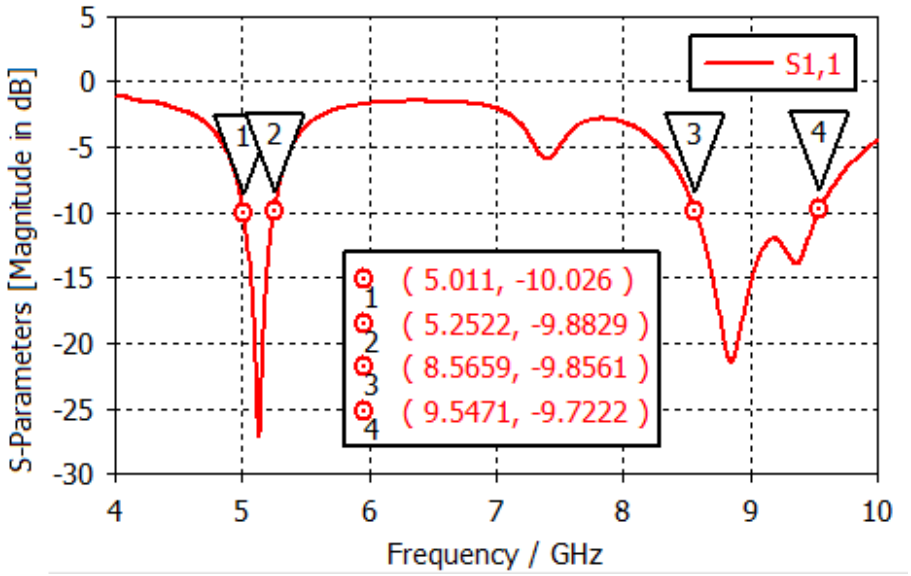

Figure 4.3 S-parameter of the proposed antenna

4.2.2 Gain and Radiation pattern

Figures 4.4 (a, b) show the radiation pattern of the proposed antenna. The antenna has a gain of 3.6 dBi at 5.2 GHz and 3.5 dBi at 8.8 GHz which is considered as a good gain for short range communication.

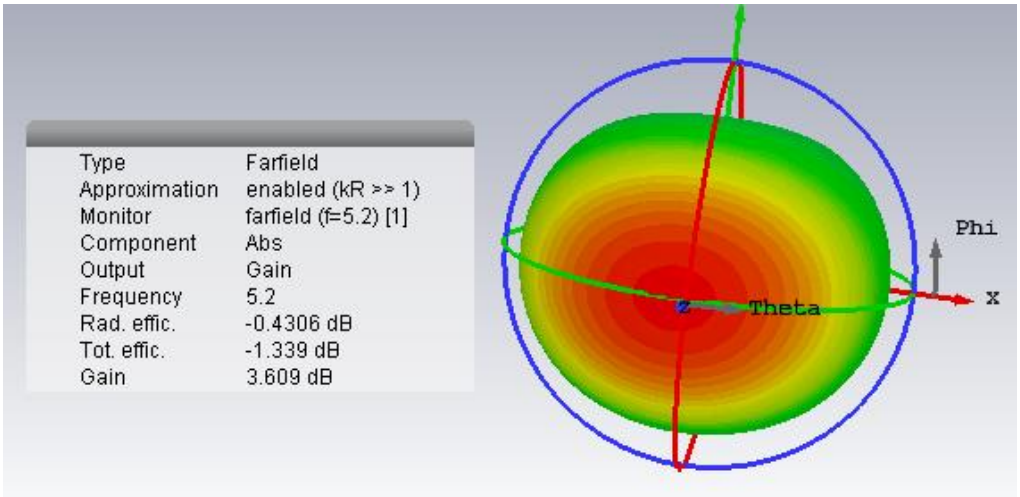

Figure 4.4 (a) Radiation pattern at 5.2 GHz

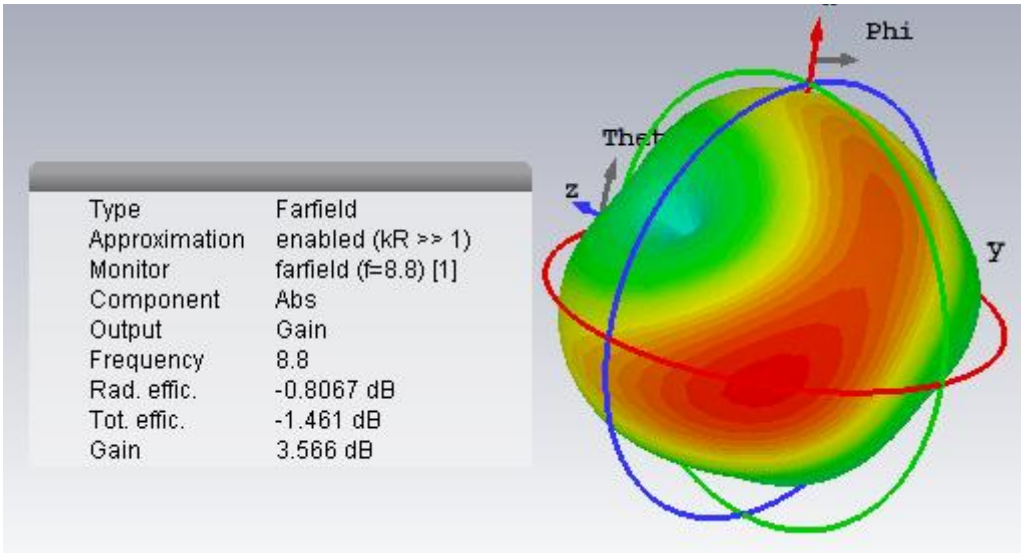

Figure 4.4 (b) Radiation pattern at 8.8 GHz

It can be seen in the figures 4.5(a, b) that the 3dB angular width is 91.8 degree along 0 degree of antenna's elevation view at 5.2 GHz and 124.7 degree along 133 degree of antenna elevation view at 8.8 GHz.

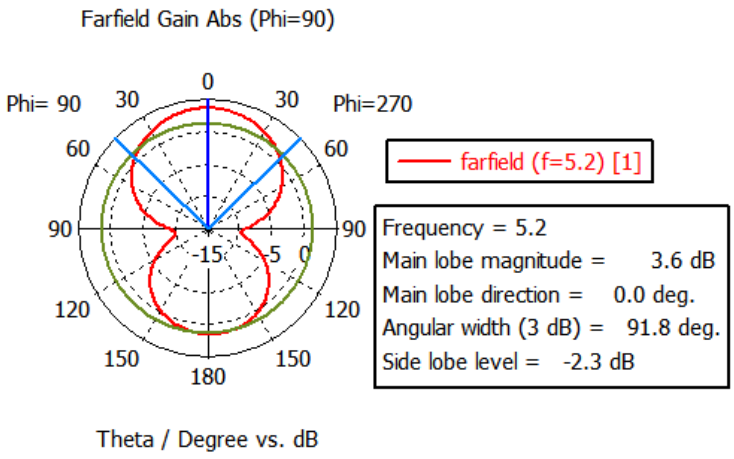

Figure 4.5 (a) Polar plot at 5.2 GHz

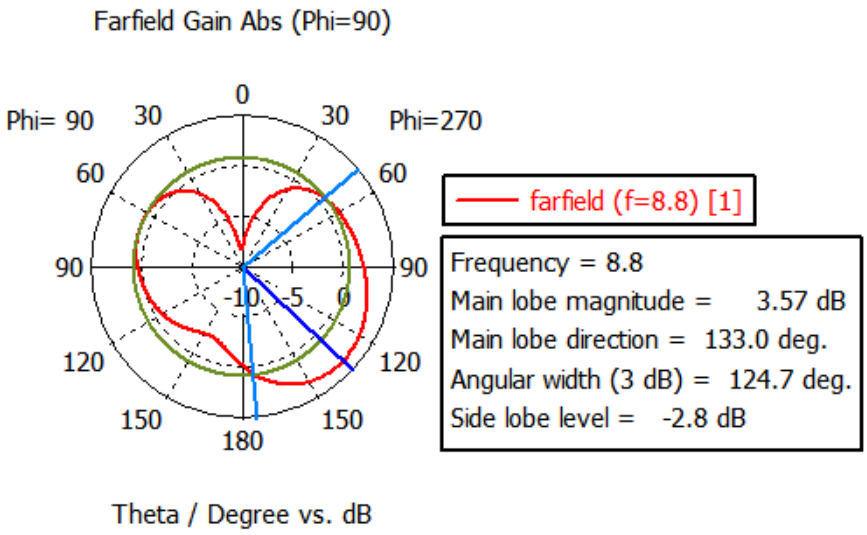

Figure 4.5 (b) Polar plot at 8.8 GHz

4.2.3 Current distribution

The Figure 4.6 (a, b) show the distribution of energy on the antenna ground surface at 5.2 GHz and 8.8 GHz, when the antenna is excited in the TE_{10} mode. Due to slots in the ground structure, current loops are formed to excite the frequency bands. A peak gain of current density of 404.8 A/m and 186.2 A/m is observed at 5.2 GHz and 8.8 GHz.

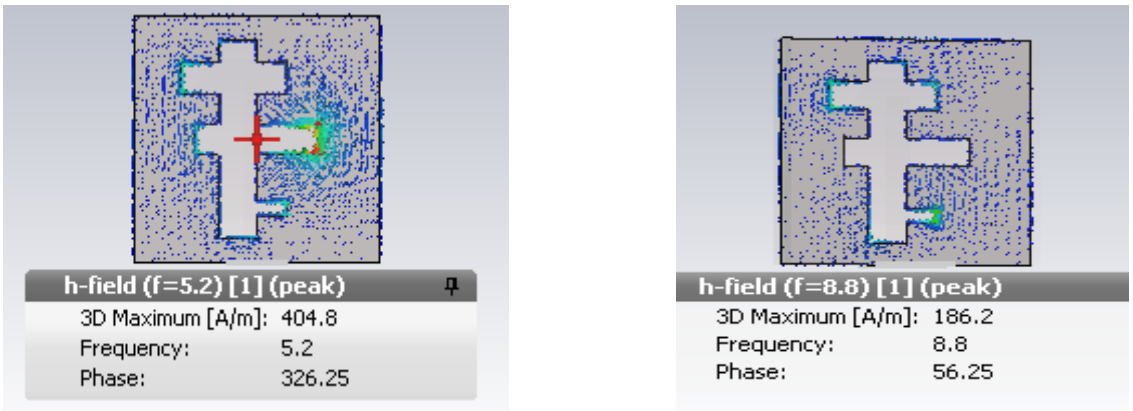

(a) (b)

Figure 4.6 (a, b) Current distribution in antenna ground at 5.2 GHz and 8.8 GHz

4.3 Design & simulation of a hexagonal MSA array for MIMO application

After getting the desired results from the designed hexagonal microstrip antenna, it is then converted into 2x2 MIMO system with two hexagonal antennas at the substrate. Figure 4.7 (a) shows the geometry of the proposed antenna. The antenna array is designed as a conventional hexagonal patch on an FR4 substrate with $\varepsilon_r = 4.4$ and h=1.57mm as The array has two feed networks ; each with its own DGS. The ground layer has a defected structure with four slots cut out

from it making a 'F' shaped slot as shown in Figure.4.7 (c). The antenna has two layers of FR4 with Regular hexagon patches having side of 6mm are designed on top of upper layer. They are $\frac{\lambda}{2}$ apart so that they don't interfere with each other. Table 4.1 mentions the detailed dimensions of the antenna array.

Figure 4.7(a) Front view of antenna

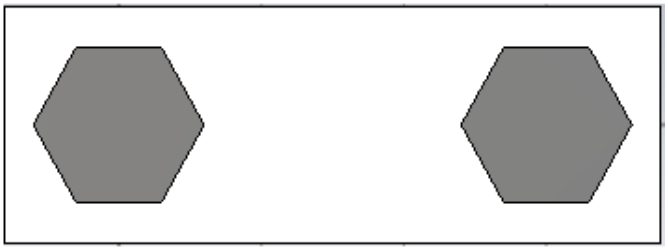

Figure 4.7(b) Top view of antenna

Figure 4.7(c) Top view of antenna ground

Table 4.1 Dimensions of optimized parameters of the proposed antenna

Parameters	**Dimensions (mm)**	**Parameters**	**Dimensions (mm)**
a	7	h	1.57
b	8.16	W_f	1.6
c	2	G_h	0.035
d	2.5	a_{eff}	6
e	13		

The proposed antenna array was simulated using CST MWS V'16 software. The designed antenna array was simulated with open boundary conditions to observe its performance for the desired wireless applications. The simulated results in terms of impedance bandwidth, broadband gain,

radiation pattern, diversity gain & ECC are presented in next section.

4.3.1 Simulation results

Antenna array simulation results are done in CST V2016 software and are mentioned in the next sub sections.

4.3.1.1 Impedance bandwidth

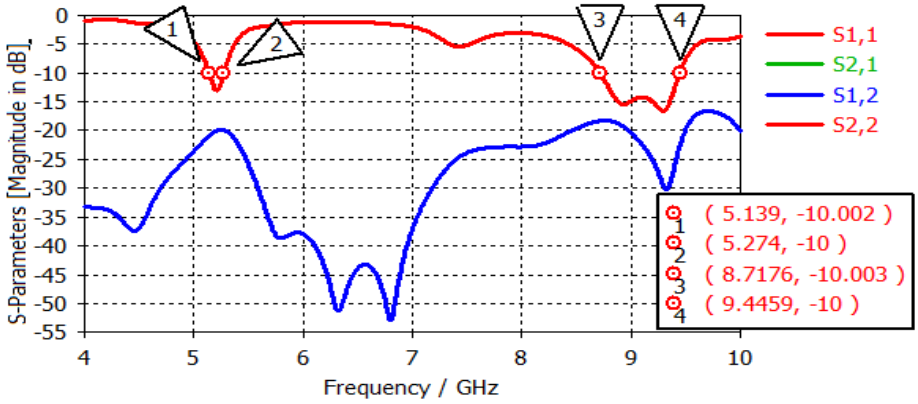

Figure 4.8 Simulated value of S-parameter

Figure. 4.8 shows the simulated results of the S-parameter for the designed Hexagonal antenna array for MIMO applications. The antenna covers two frequency bands from (5.139-5.274) GHz having bandwidth of 135MHz and (8.7176-9.4459) GHz having bandwidth of 728.3MHz. The hexagonal antennas in the array show S_{12}/S_{21}<20dB, thereby showing least interference towards each other while radiation.

4.3.1.2 Current Distribution

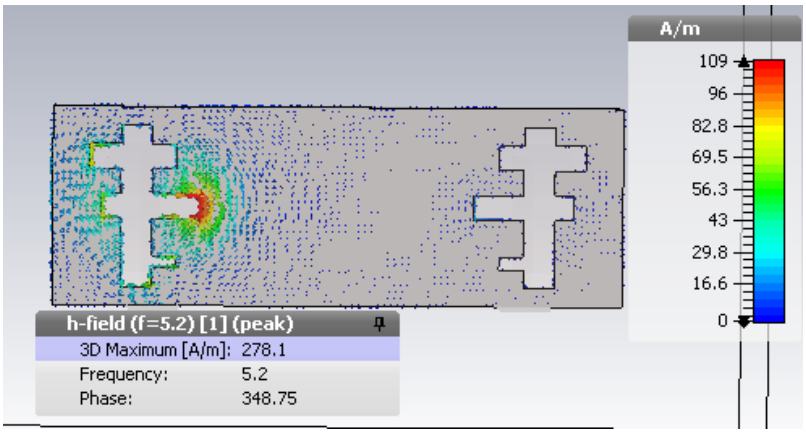

Figure 4.9 Current distribution at 5.2GHz

The Figure 4.9 shows the distribution of energy on the antenna ground surface at 5.2 GHz when the antenna is excited in the TE_{10} mode. Due to slots in the ground structure, current loops are formed to excite the frequency bands. A peak current density of 109 A/m is available on the antenna ground layer at 5.2GHz.

4.3.1.3 Radiation Pattern and Gain

Figure 4.10 shows the broadband gain of the proposed antenna array. The designed array shows average gain of 3.5dB (approx.) for the entire band. Figures 4.11(a, b) show the radiation pattern of the antenna at 5.2 GHz and 9.2 GHz respectively .The antenna peak gain is 4.6dB at 8.71 GHz frequency of operation.

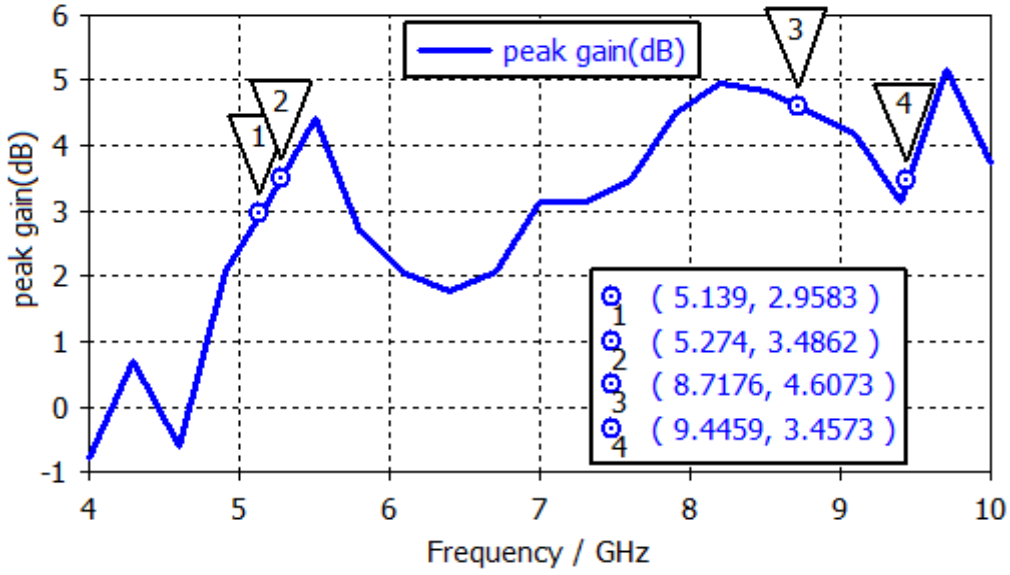

Figure 4.10 Gain over the entire bandwidth

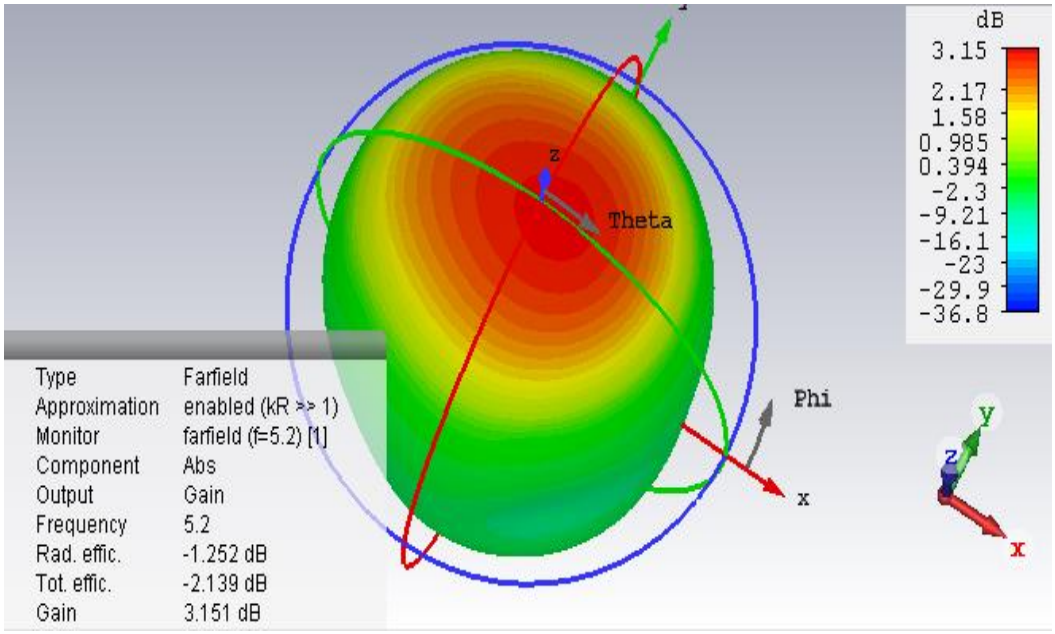

Figure 4.11(a) Radiation pattern at 5.2GHz

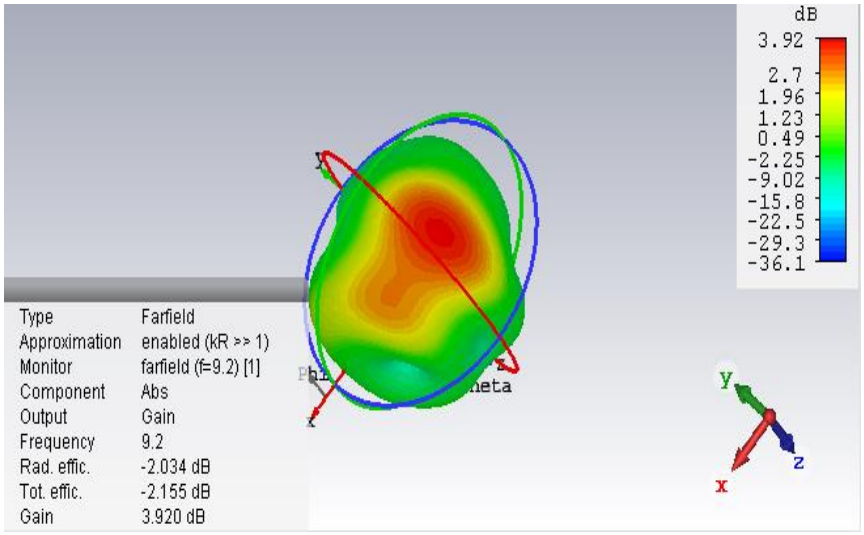

Figure 4.11(b) Radiation pattern at 9.2 GHz

Polar plots convey the information about the antenna directivity, the major and minor lobes and half power beamwidth. It can be seen in the figures 4.12(a, b) the 3dB angular width is 101.8 degree along 1 degree of antennas elevation view at 5.2 GHz and 69.3 degree at the frequency of 9.2 GHz.

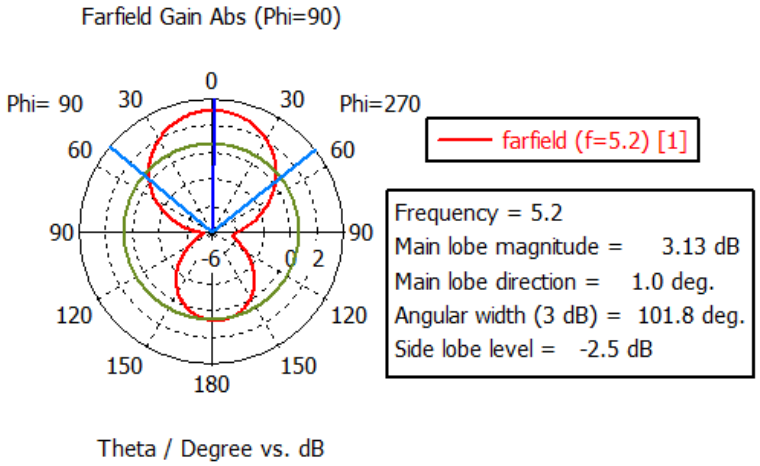

Figure 4.12 (a) Polar plot at 5.2GHz

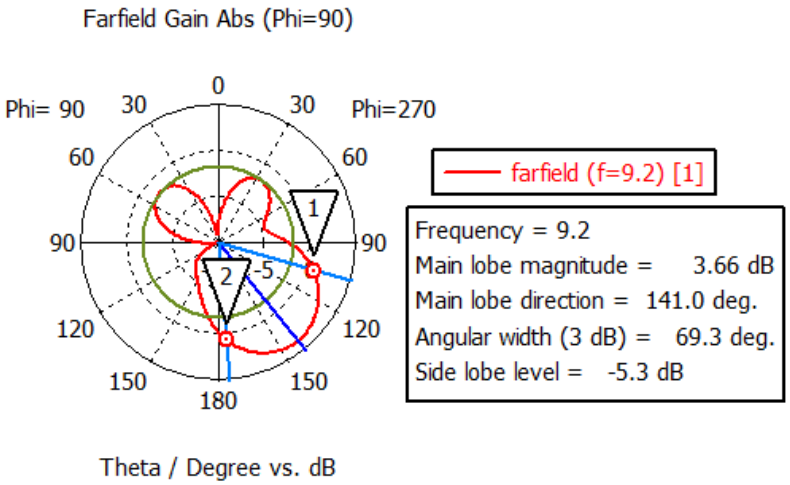

Figure 4.12(b) Polar plot at 9.2 GHz

4.3.1.4 ECC

In MIMO antennas, correlation coefficient is a major concerned parameter as it gives the information about how antennas are interfering with each other while radiation. The ECC can be calculated by using S-parameters by using the equation 4.4 for a 2x2 antenna system.

$$ECC = \frac{|S_{11}^{*}S_{22}+S_{21}^{*}S_{12}|^{2}}{(1-|S_{11}|^{2}-|S_{21}|^{2})(1-|S_{22}|^{2}-|S_{12}|^{2})} \tag{4.4}$$

The ideal value of the ECC is zero but practically value of the uncorrelated MIMO antenna should be ECC<0.5. The value of the ECC for the designed antenna is ECC<0.0034 as shown in Figure. 4.13 for the entire UWB which is very good as it close to zero.

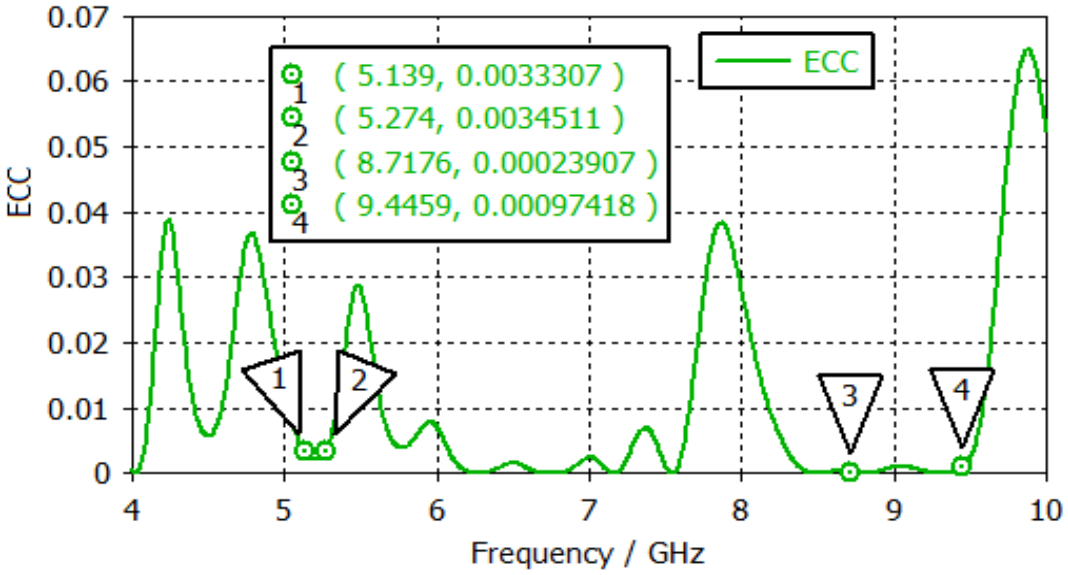

Figure 4.13 ECC for the proposed antenna array

4.3.1.5 Diversity Gain

Diversity gain (DG) is another parameter which is taken care of while designing MIMO antennas. The performance analysis of a MIMO array is done using this parameter and it is given by the equation 4.5

$$DG = 10\sqrt{1-(ECC)^{2}} \tag{4.5}$$

With an extra receive antenna, the probability of error decreases with SNR at the rate of SNR^{-2}. Since the performance gain at high SNR is dictated by the SNR exponent of the error probability, this exponent is called the diversity gain. A good diversity gain is demanded for high data rate MIMO applications. figure 4.14 shows the plot of diversity gain of the antenna, a peak diversity gain of 9.99is exhibited by the antennas of the array at a frequency of 8.71GHz.

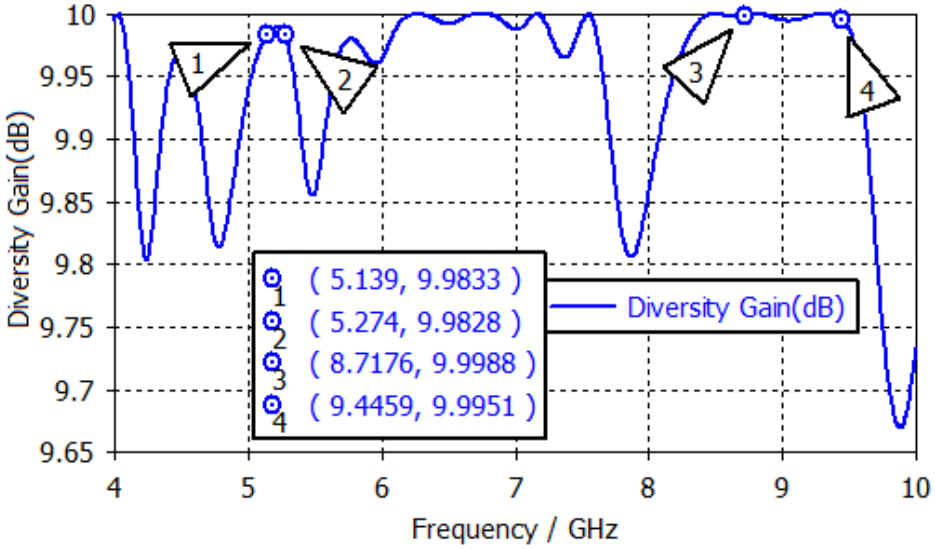

Figure 4.14 Diversity Gain

4.4 CONCLUSION

This chapter presents a hexagonal MSA & then its design is extended to a compact hexagonal microstip antenna array for IEEE 802.11, X-band wireless applications. The proposed antenna array shows a dual band behavior for frequencies between (5.139-5.274) GHz and (8.71-9.44) GHz. Antenna array shows an average gain of 4.14dB over entire band of operation that suits short range applications. A low correlation coefficient of ECC<0.0034 allows the two antennas to be uncoupled when used for WLAN MIMO applications, thereby not providing interference to each other. The antenna has high diversity gain which is prime requirement of a MIMO system to support high data rate applications.

CHAPTER 5

DESIGN AND SIMULATION OF A FSS BASED FRACTAL MSA FOR WLAN APPLICATIONS

Frequency selective surfaces (FSS) are specially designed to provide a selective behavior to certain frequencies. These surfaces allow only the desired frequencies to pass through and reject the unwanted ones [48]. Fractal antennas are discussed in detail in the previous chapters, these were used to design Antenna Arrays for MIMO applications. In this chapter the fact that multiband properties of fractals shapes can be favorably useful to design multiband frequency selective surfaces (FSS) has been utilized. This chapter presents a Sierpinski dipole FSS based antenna to get a dual band behavior for resonant frequencies of 3.7 GHz, 7 GHz and a stop band from 7.8 GHz to 10 GHz frequency range. The antenna is thus suitable for WLAN applications with desired pass and stop bands.

5.1 THEORETICAL ANALYSIS

The use of frequency selective surfaces has been successfully proven as a mean to increase the communication capabilities of satellite based communication systems. In space missions such as Voyager, Galileo and Cassini the use of dual-reflector antennas with a sub reflector made of an FSS has made it possible to share the main reflector among different frequency bands by eliminating the interference from nearby bands [49, 50].

In context to the FSS designing, a Sierpinski dipole derived from a Sierpinski gasket fractal is designed in this chapter. The basic Sierpinski gasket is iterated upto three levels and is constructed by subtracting a central inverted triangle from the original triangle for the 1st iteration. More triangles which are scaled down versions of the original triangle are cut at every iteration upto three levels to get the final sierpinski gasket fractal. Two sierpinski gasket fractals are joined at the apex with the help of a dipole at the center. In order to get a selective frequency response, the height of each sierpinski gasket FSS should be at least 2h which is related to the frequency of operation by the equation 5.1. The distance between the centers of two FSS designed should be at least dx_1 In order to keep the radiators from overlapping dy has to be greater than $2 * h$ Equations 5.1 and 5.2 should be satisfied to get the desired passbands and stop bands respectively.

$$2\frac{h}{\lambda_1} = 0.306 \tag{5.1}$$

$$2\frac{h}{\lambda_2} = 1.032 \tag{5.2}$$

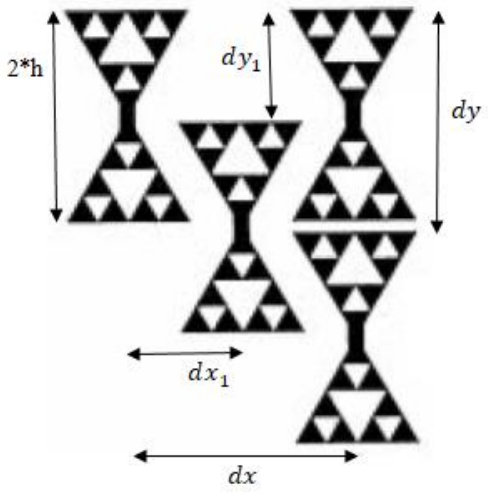

Figure 5.1 Sierpinski dipole patch

$$dx = dy = 2 * dx_1 = 2 * dy_1 \tag{5.3}$$

$2 * h$ Is the total height of the Sierpinski dipole.

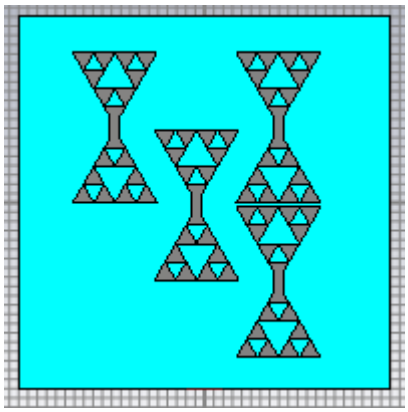

Figure 5.2 Front view of antenna

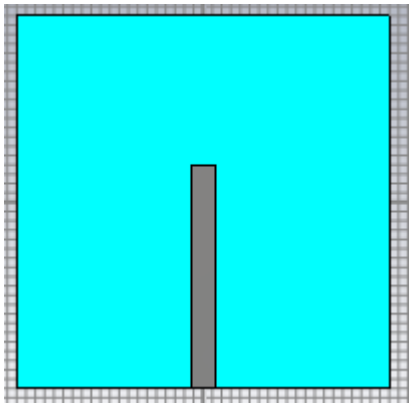

Figure 5.3 Back view of antenna

The antenna is designed on an FR4 substrate and it is also excited using aperture coupled feed. The ground has a defected structure and a rectangular loop is created in the ground structure which provides a feature of band notch filtering from 7.8 GHz to 10.3 GHz. The radiators are also scaled to

get the desired optimized results. Figures 5.2 and 5.3 show the snapshots of the designed antenna and its feed network.

5.2. ANTENNA SIMULATION RESULTS:

The antenna was simulated using CST MWS V 2016 software and the simulated results in terms of S parameters, gain and current distribution are measured and presented in next subsections:

5.2.1. Return Loss and Antenna Bandwidth

Figure 5.4 shows the graph between return losses versus frequency plot of the proposed antenna. It's covering a dual band ranging from (3.679-3.756) GHz with a bandwidth of 77 MHz and (6.438-7.873) GHz with bandwidth of 1.435 GHz. This frequency covers WLAN and Wi-MAX wireless applications successfully.

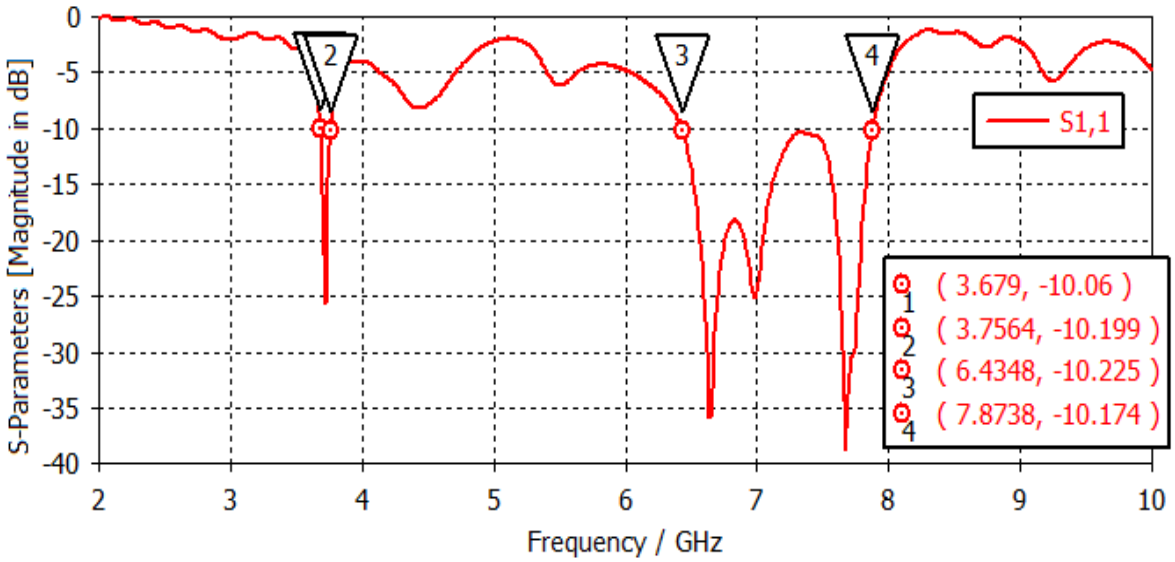

Figure 5.4 Return Loss S11 (dB) v/s Frequency Plot of antenna

5.2.2 Current Distribution

The current distribution results when the FSS based antenna was excited are given in figure 5.5(a, b) for two desired resonant frequencies of operation. The ground layer shows a maximum current distribution of 90.9 A/m at frequency of 7 GHz & the FSS patch shows a peak current of 235.3 A/m on the patches at a frequency 3.7 GHz.

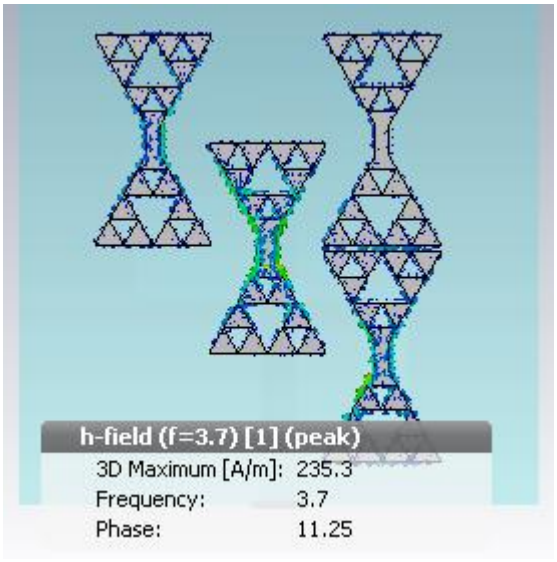

(a)

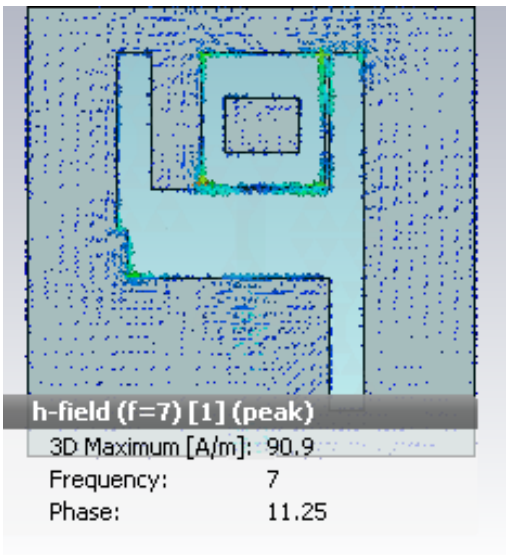

(b)

Figure 5.5 (a, b) Current distribution at 3.7 GHz and 7 GHz

5.2.3. Radiation Pattern and Gain

Figures 5.6(a, b) show the radiation plot of the simulated antenna designed for broadband applications. The antenna shows a total radiation efficiency of -2.453dB at 3.7GHz and a radiation efficiency of -0.727dB at 7GHz. The proposed antenna has a peak gain of 4 dBi at 7.5 GHz.

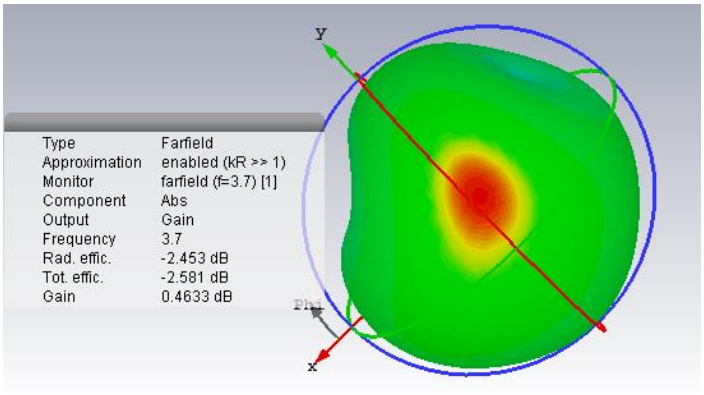

Figure 5.6 (a) Radiation pattern at 3.7 GHz

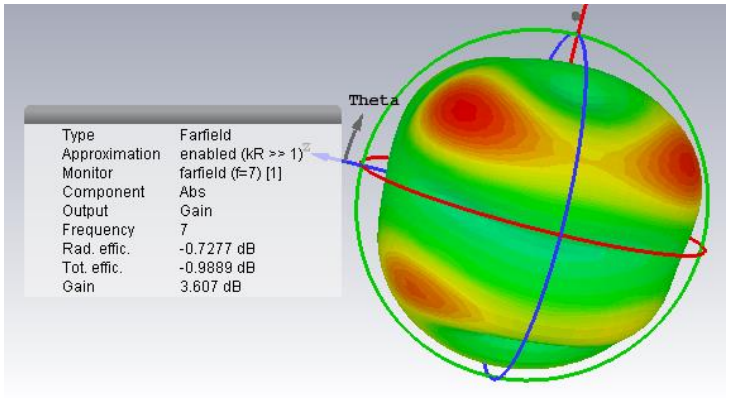

Figure 5.6 (b) Radiation pattern at 7 GHz

Polar plots are the 2D plots of antenna's radiation pattern. It shows the pattern of lobes i.e. maxima and minima of the antenna radiation. Figures 5.7(a, b) shows the polar plots at the two resonating frequencies.

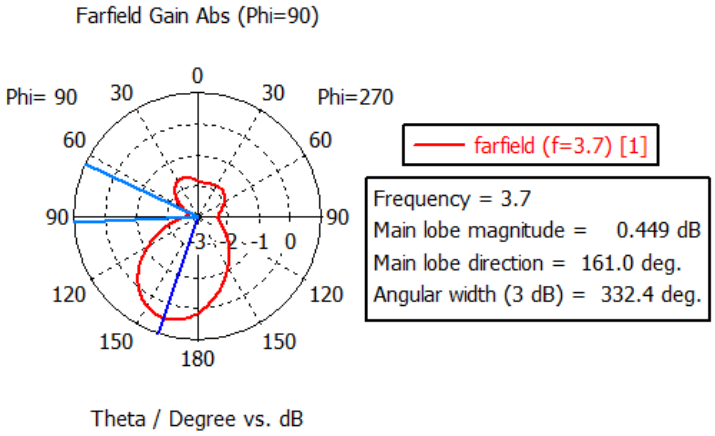

Figure 5.7 (a) Polar plot at 3.7 GHz

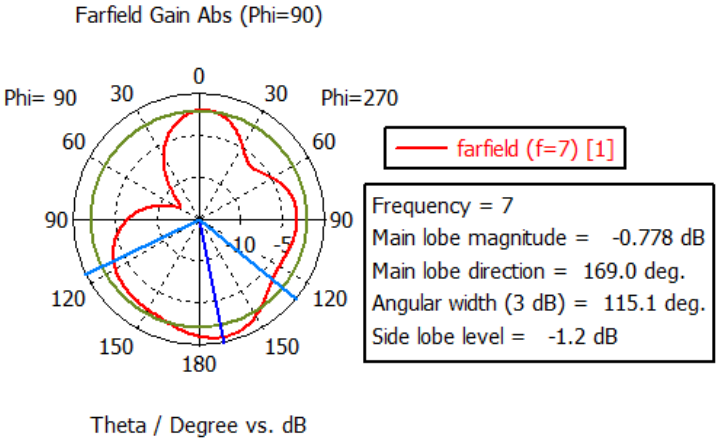

Figure 5.7 (b) Radiation pattern at 7 GHz

Figure 5.8 shows the broadband gain of the antenna with the peak gain of dBi at the desired frequency band of operation.

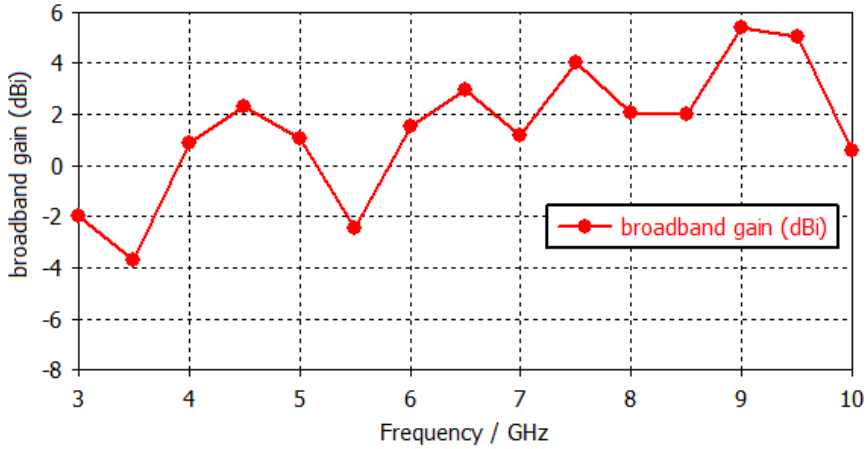

Figure 5.8 Broadband gain of the proposed antenna

5.3. CONCLUSION

This chapter presented a FSS (frequency selective surface) based antenna with a dual band at resonant frequencies of 3.7 GHz and 7 GHz and having a band notch property from 7.8 GHz to 10.3 GHz.. The antenna shows frequency selective properties and it is made from eight triangular sierpinski gasket fractals that are joined at the apex with a dipole. The proposed antenna shows an impedance bandwidth of 79.4 MHz and 1.439 GHz for the bands (3.7564-3.677) GHz and (7.8738-6.4348) GHz .It is suits the wireless applications of WLAN and Wi-MAX.

Chapter 6

FABRICATION AND TESTING OF DESIGNED ANTENNA

This chapter presents the fabrication process and the testing results of the two fabricated antenna designs i.e. 2 x 2 sierpinski triangular gasket fractal antenna and FSS (frequency selective surface) antenna which are designed and simulated in chapter 3 and 5. The antennas are fabricated on FR4 substrate using photolithography (wet etching) process. Here, return loss for both the antennas are measured using Agilent's vector analyzer (VNA) model no. E5063A and E5071C, having operating frequency range from 1 to 20 GHz and 9 KHz to 8.5 GHz respectively.

The antenna fabrication process involves a few steps which are mentioned in detail in the next section

6.1 FABRICATION PROCESS

The flow chart of the antenna fabrication is given below

Table 6.1 Antenna fabrication process

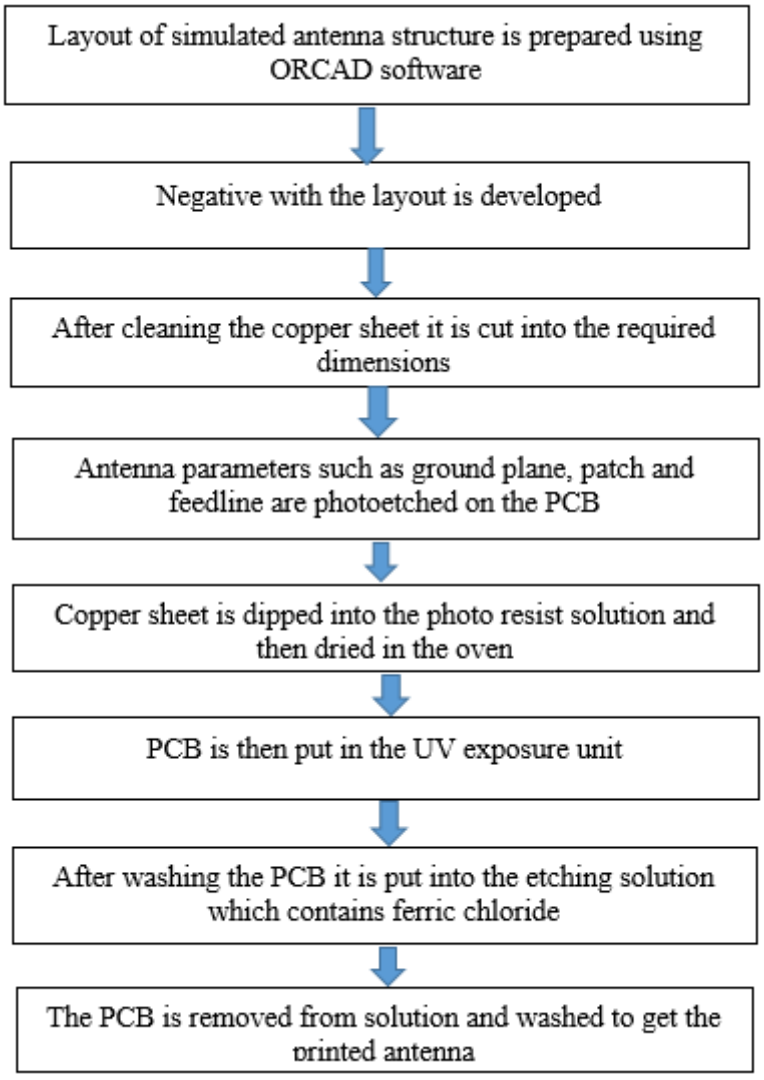

After the antenna fabrication process the above mentioned antennas were tested for S-parameter bandwidth using a vector network analyzer.

6.2 VNA

VNA stands for vector network analyzer it is used to testing components for practical purposes. The most important concept of a high-frequency network analysis involves incident, reflected and transmitted waves travelling along the transmission lines. A network analyzer is an instrument used to measure impedance. At lower frequencies, the impedance with relatively simple tools can be measured, including a sine wave generator, a volt meter, a current meter, and a calculator. Using these tools, the ratio between voltage and current can be measured and the resulting impedance can be calculated. In this thesis two VNA models were used i.e. KEYSIGHT E5063A and E5071C. E5063A have a frequency range from 100 KHz to 18 GHz and E5071C have a frequency range on 20 KHz to 8.5 GHz. figure 6.1 shows the E 5063 VNA used for testing of antennas.

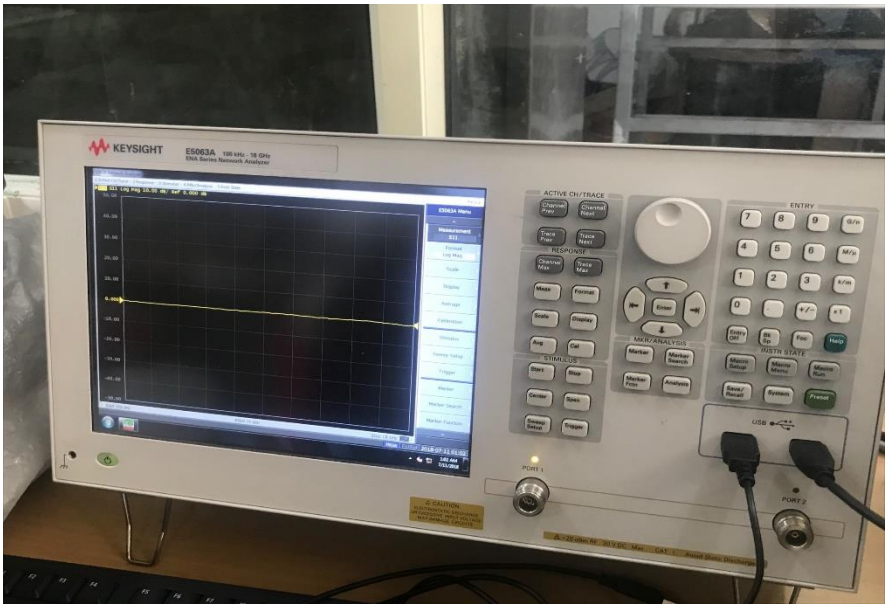

Figure 6.1 Vector Network Analyzer

6.3 TESTING OF TRIANGULAR SIERPINSKI GASKET FRACTAL ANTENNA ARRAY

The testing of the FSS based triangular sierpinski gasket fractal a fabricated antenna has been done by using VNA model no E5071C whose frequency range is from 20 kHz to 8.5 GHz. Figure 6.2 shows the prospective view of the fabricated antenna and Figures 6.3(a, b, c) show the different layers of the designed antenna i.e. Antenna patch, ground and stripline respectively.

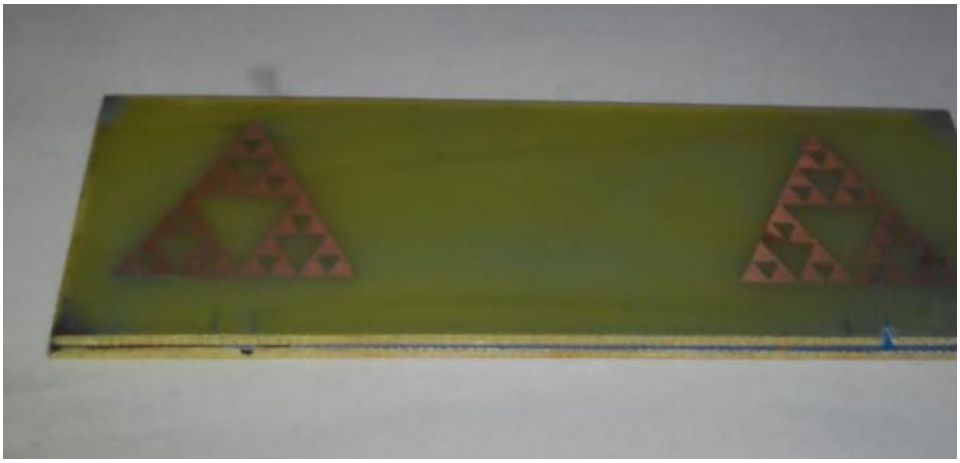

Figure 6.2 Snapshot of the assembled triangular sierpinski gasket fractal antenna array

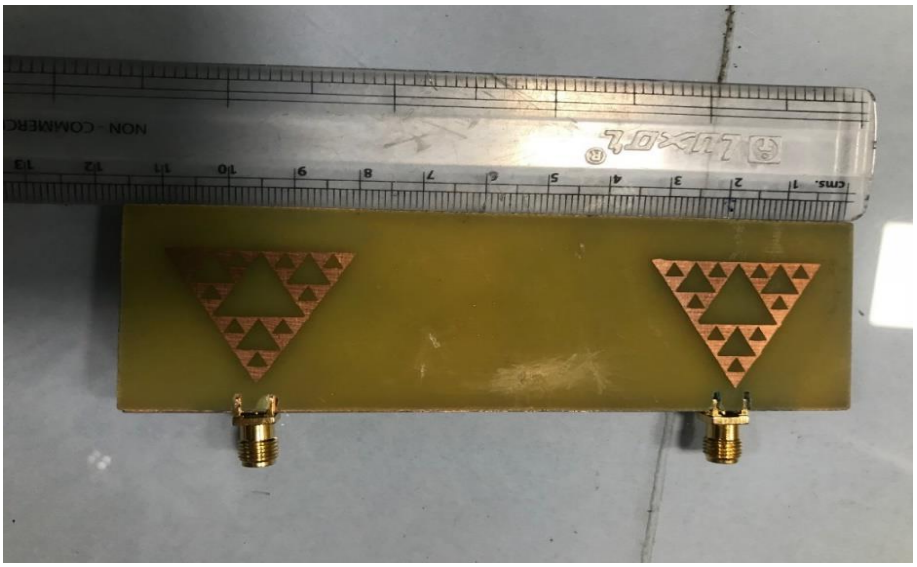

(a) Triangular sierpinski gasket fractal Antenna patches in the array

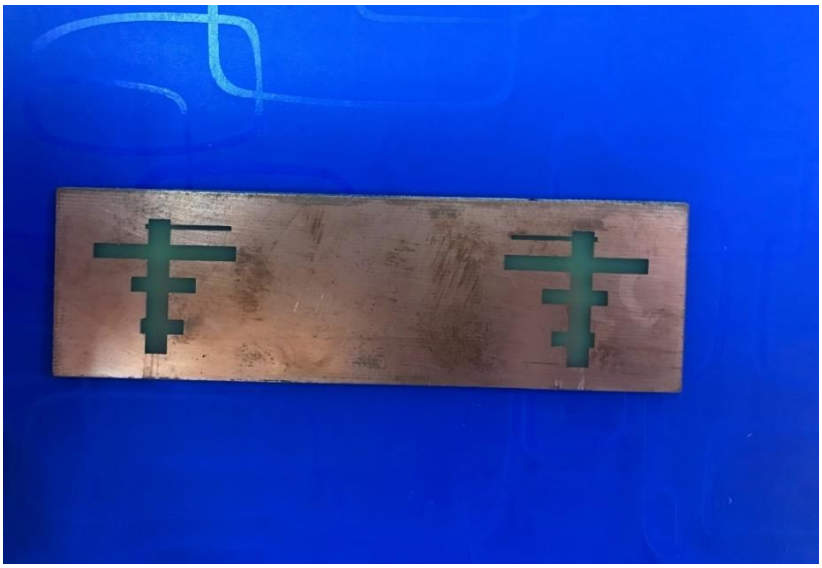

(b) Antenna ground shows a DGS

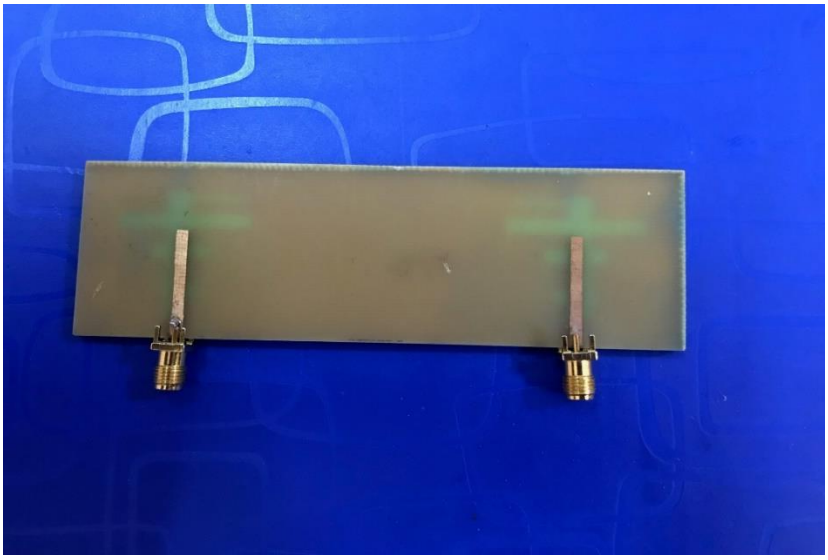

(c) Feed network of the array with two striplines

Figure 6.3 (a, b, c) show the three individual layers of the antenna array

6.3.1 Measurement Results

The comparison graph of the simulated results and the measured results of return loss are shown in figures 6.4(a-d) and 6.5(a - d). Figure 6.4 (a) shows the snapshot of antenna testing for S_{11} on a VNA and Figure 6.4(b) shows the comparison between simulated and measured S_{11} results for the proposed antenna array. An UWB was observed in the simulated result which was covering a range from (5.48-6.48) GHz but in the measured results there are multi bands which are covering two resonant bands in measured results covering a bandwidth of (5.6-5.8) GHz and (6.3- 6.6) GHz which can be used for WLAN band. A reason for this shift can be because of the errors introduced during the fabrication process.

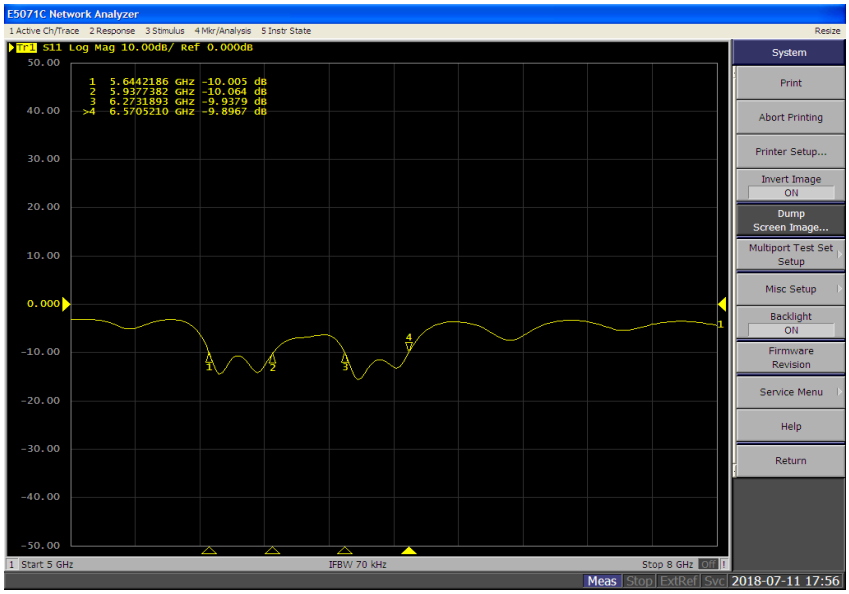

Fig 6.4(a) Snapshot of S_{11} testing on the VNA

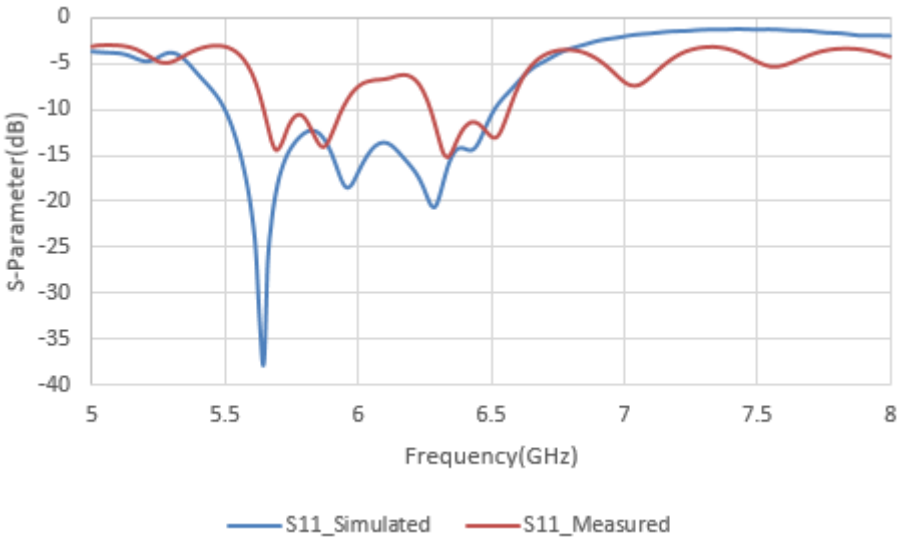

Figure 6.4 (b) S_{11} Comparision graph of simulated and measured

Figure6.4(c) shows the snapshot of S_{22} testing on a VNA. Figure 6.4(d) shows the comparative plot between the simulated and measured S_{22} parameter. The simulated results show a frequency band covered from 5.48 GHz to 6.48 GHz. It is seen that the measured results are right shifted in the frequency range as compared to the simulated results. The frequency range from (5.6-5.7) GHz, (6.3-6.4) GHz (6.7-7.5) GHz with bandwidth of 100 MHz, 100 MHz and 50 MHz which can be used for WLAN and C-band applications successfully.

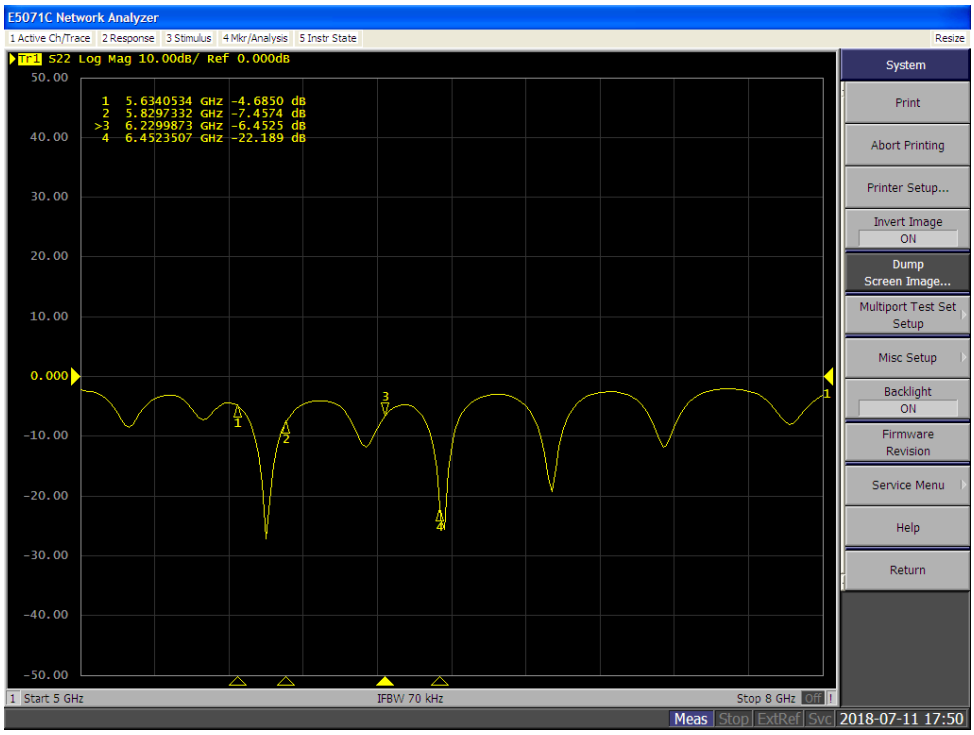

Figure 6.4 (c) Snapshot of measured S_{22}

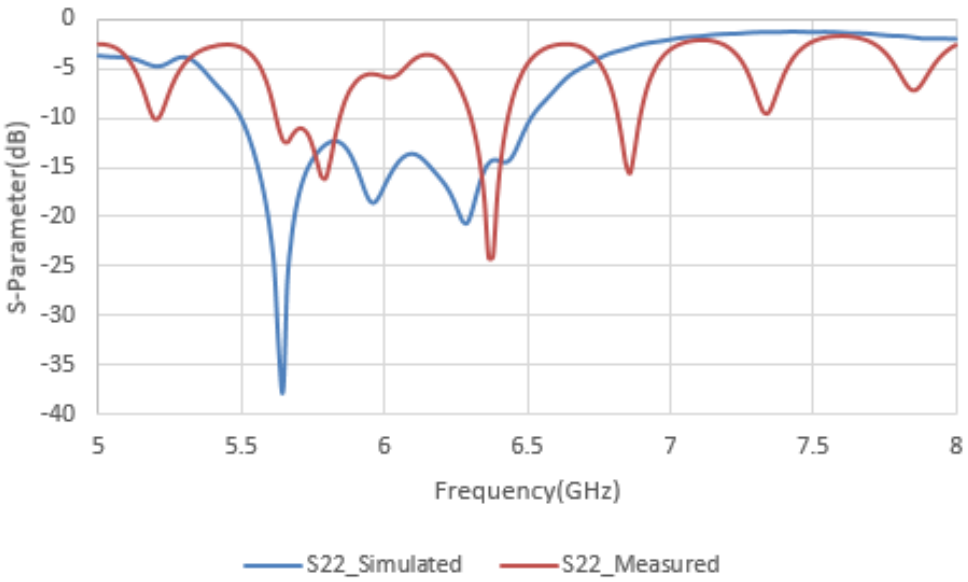

Figure 6.4 (d) Comparison of simulated and measured S_{22} parameter of the antenna array

Figures 6.5 (a, b, c d) show the snapshots of $S_{21}$and S_{12} on the VNA screen and the comparison of simulated and measured S_{21} and S_{12} results. It is observed from the figure 6.5 (c, d) that he measured results and the simulated results are both lie under -20 dB which means both are antennas in the proposed antenna array are independently radiating and are not interfering with each other while transmission/Reception.

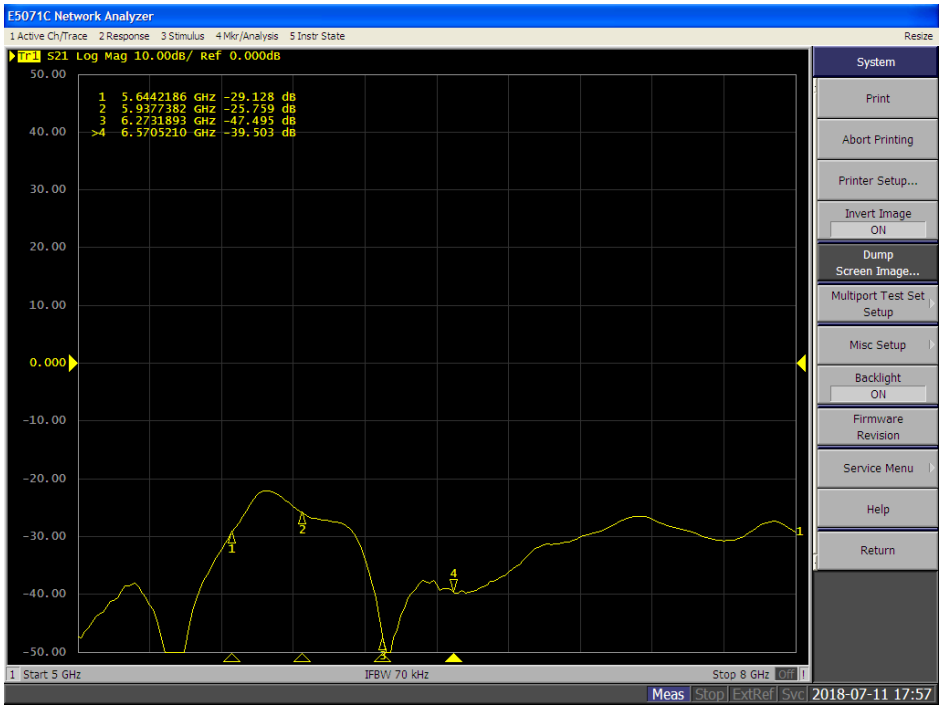

Figure 6.5 (a) Snapshot of measured S_{21}

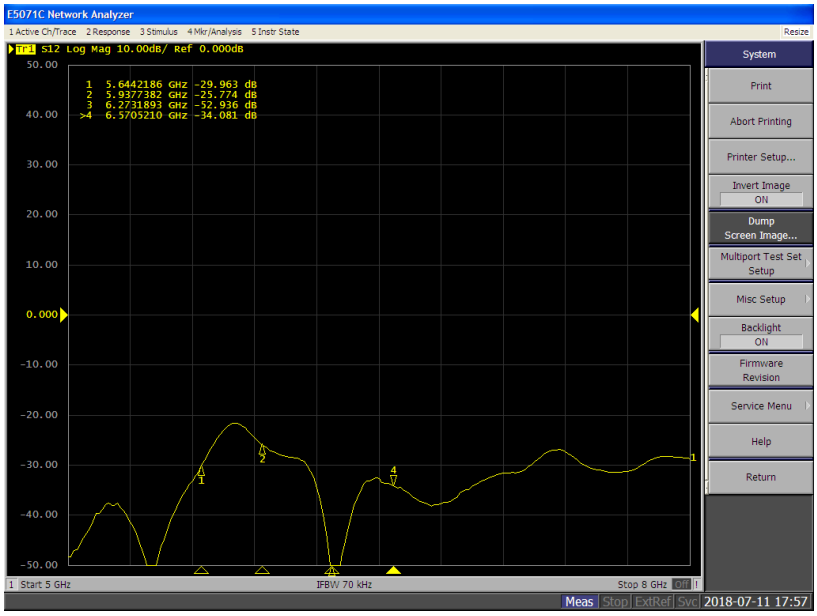

Figure 6.5 (b) Snapshot of measured S_{12}

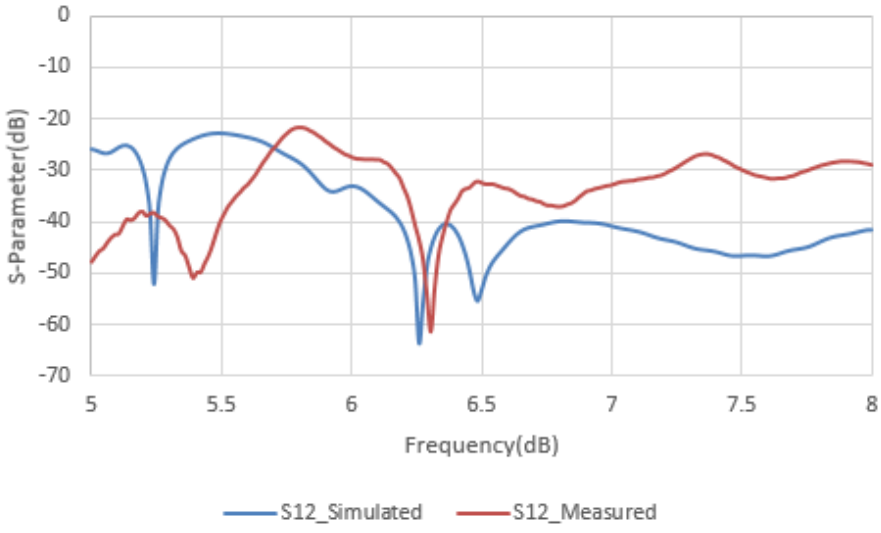

Figure 6.5 (c): Comparison between simulated and measured S_{12}

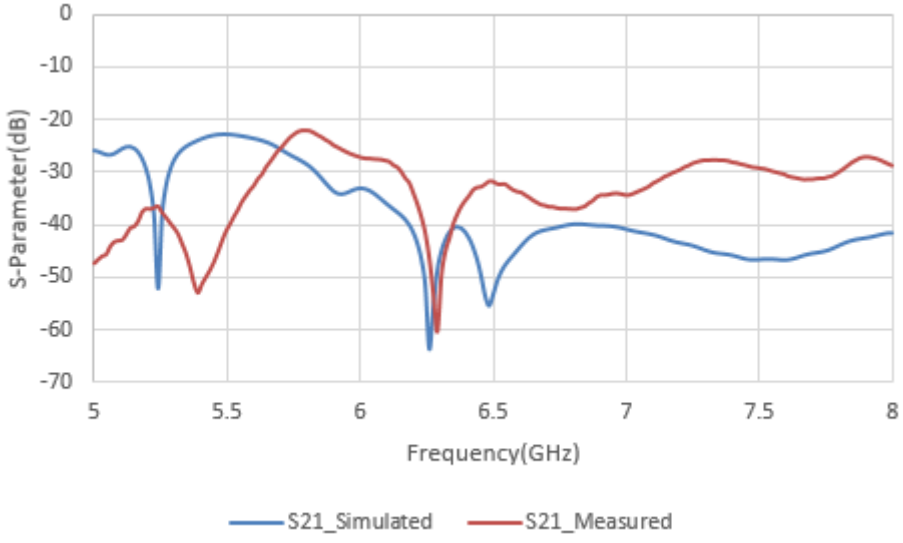

Figure 6.5 (d): Comparison between simulated and measured S_{21}

Table 6.2 Summarizes the simulated and measured results of the triangular sierpinski gasket fractal antenna array

S. No.	**Parameter**	**Simulated Results**				**Measured**			
		Return freq (GHz)	Return loss (dB)	Impedance bandwidth (MHz)	Wireless Applica-tion	Resonant freq (GHz)	Return loss (dB)	Impedance bandwidth (MHz)	Wireless Application
1.	S_{11}	5.62	-45	1006	WLAN, C-band	5.7,5.9, 6.4	-14, -14, -15	200, 300	WLAN, C-band
2.	S_{22}	5.62	-45	1006	WLAN, C-band	5.8, 6.4, 6.8	-16, -24, -15	100, 100, 50	WLAN, C-band

6.4 TESTING OF FSS BASED FRACTAL ANTENNA

The testing of the fabricated antenna has been done by using VNA model no E5063A (Agilent Technologies), whose operating frequency range is from 100 kHz to 18 GHz. The antenna was fabricated using the process mentioned in table 6.1 and figure 6. 6 (a-d) show the snap shots of antenna geometry and its various layers.

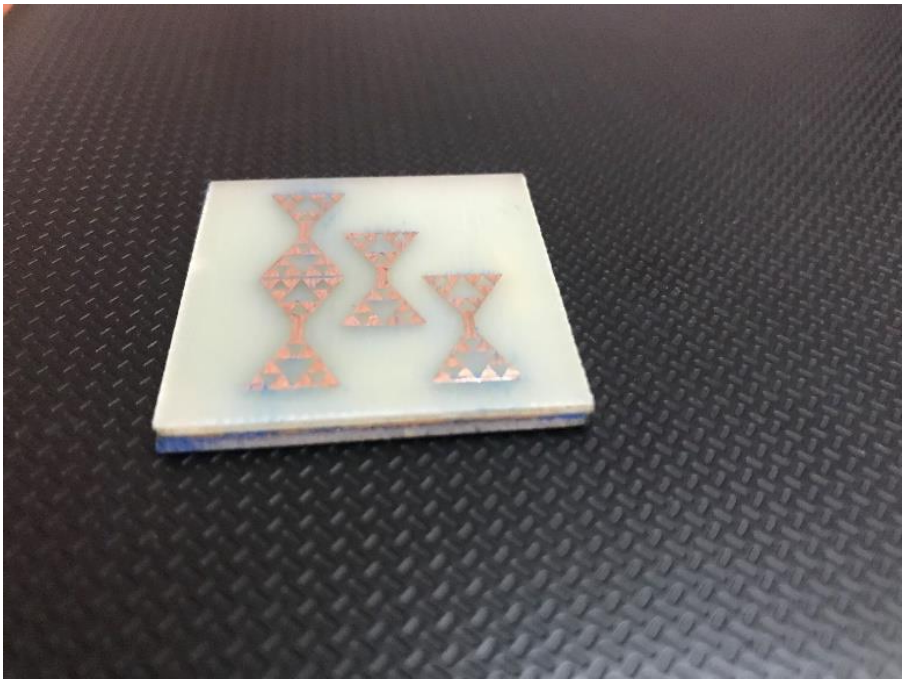

Figure 6.6 (a) Snapshot of the assembled FSS based aperture coupled antenna

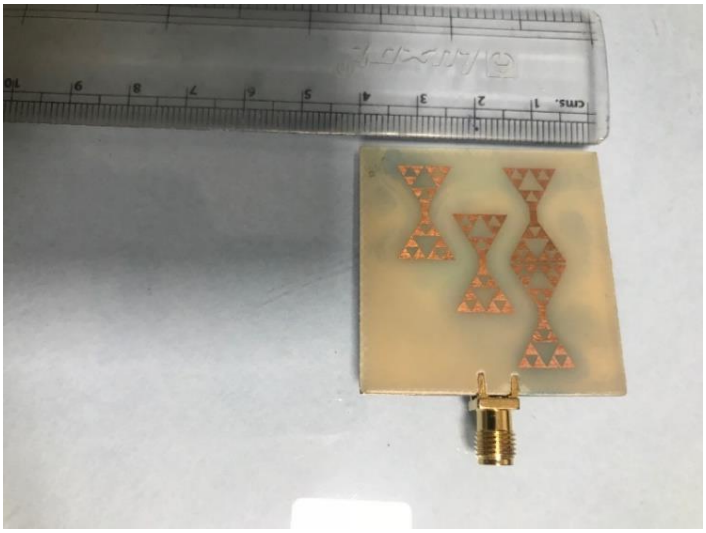

(b) Antenna patch

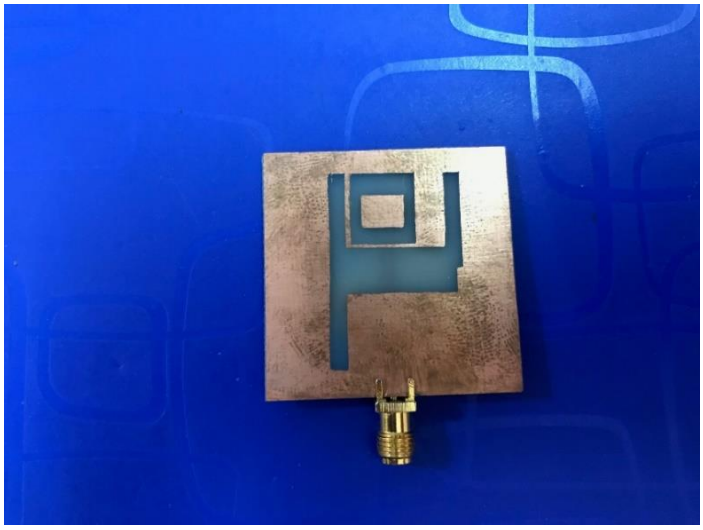

(c) Ground structure

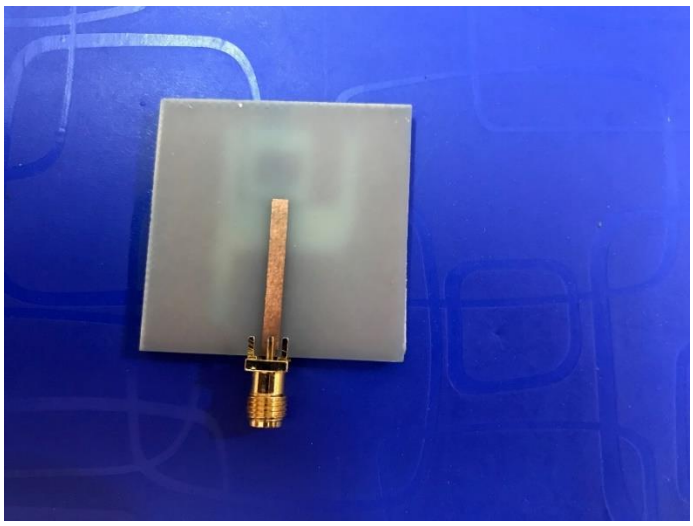

(d) Stripline

Figure 6.6 (b, c, d) Snapshot of different layers of the antenna FSS based aperture coupled antenna

6.4.1 Measurement Results

Figure 6.7 (a, b) show the snapshots of the antenna testing on VNA and a comparison graph between simulated and measured S-parameter results of the antenna respectively. It can be seen that the measured results are almost same as the simulated results. The antennas shows a simulated frequency band from 6.44 GHz to 7.88 GHz And the measured results show that the antenna is covering a dual band from 3.9-4 GHz with bandwidth of 100 MHz and 5.8-8.3 GHz with bandwidth of 2.5 GHz covering the application of WLAN, C-band and X-band. A small variation in the measurement results is seen and the reason for this can be because of the errors introduced during the fabrication process.

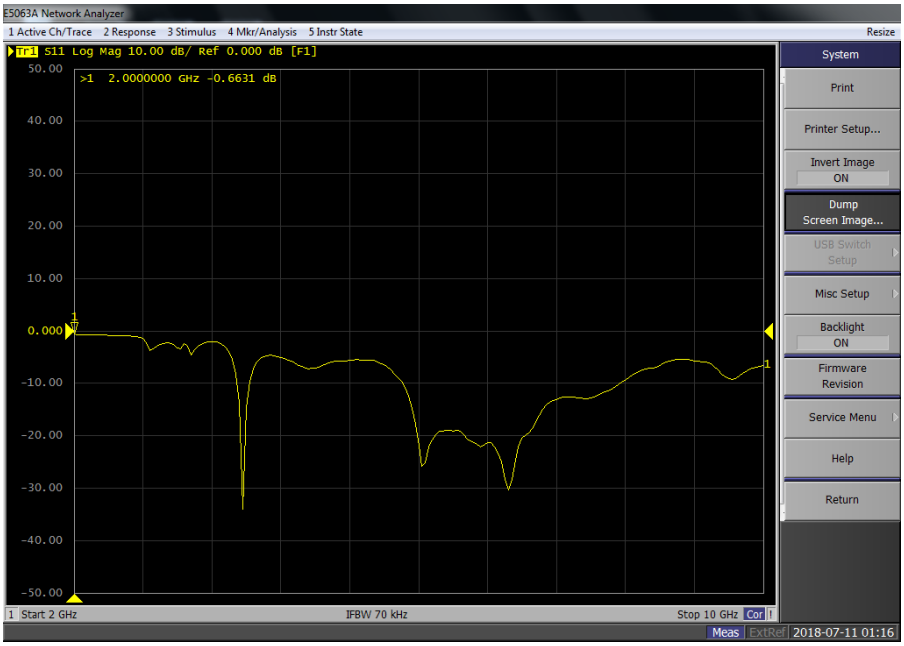

Figure 6.7 (a) Snapshot of measured S_{11}

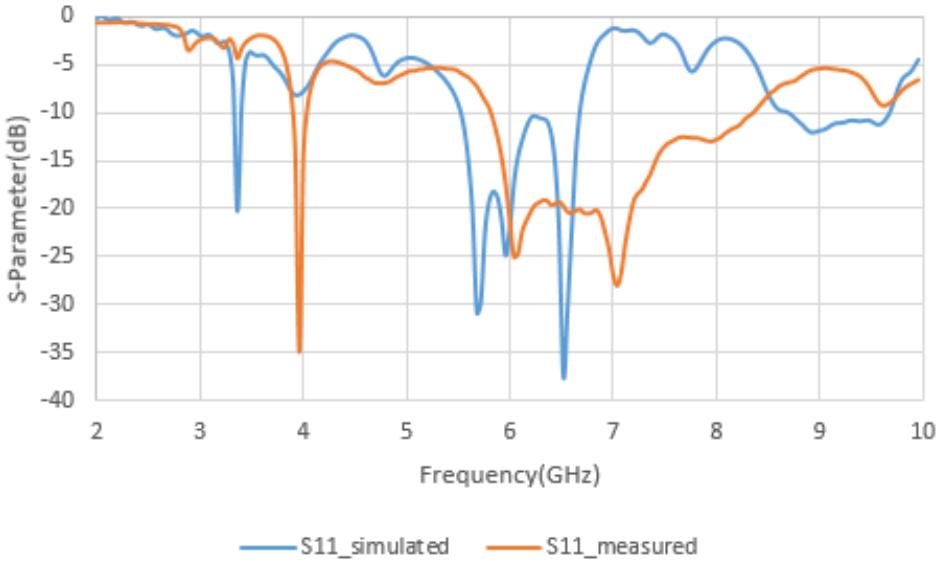

Figure 6.7 (b) Comparison of simulated and measured results

Table 6.3 Summarizes the simulated and measured results of the proposed FSS based antenna array

Simulated Results				**Measured**			
Return freq (GHz)	Return loss (dB)	Impedance bandwidth (MHz)	Wireless Application	Resonant freq	Return loss (dB)	Impedance bandwidth (MHz)	Wireless Application
3.7, 7	-25, -25	77.4, 1439	WLAN, C-band	4, 6.1, 7.1	-35, -25, -27	100, 25000	WLAN, C-band and X-band

6.5 CONCLUSION

This chapter presented the fabrication and testing of a triangular sierpinski gasket fractal antenna array and a triangular sierpinski gasket FSS based antenna. The antennas measurement results are found to be matching with the simulated ones and the two proposed antennas are well suited for Wi-Fi and RFID practical wireless applications.

CHAPTER 7

CONCLUSION AND FUTURE SCOPE

The research work presented in this thesis started with the study on aperture coupled Microstip Antennas and their designing. Since fractal antennas have a property that they show multiband properties and with defected ground structures (DGS), these nearby bands can be overlapped to show wideband behavior; the next research was carried out in the field of fractal MSA with DGS. Aperture coupled fractal MSA were designed and their performance was evaluated using CST MWS V'16 software.

MIMO antennas are greatly in demand these days to combat fading and multipath interference. These require antenna arrays that can work on a specific frequency band to be implemented as a MIMO system.

Therefore the research work carried out in the field of fractal MSA was then extended to MIMO systems. A triangular sierpinski gasket fractal antenna array and hexagonal antenna array with aperture coupled feeding was designed and evaluated for S parameters, ECC and Diversity gain.

Some wireless applications require the desired frequency bands to be separated by stop bands to eliminate interference, therefore the next research work presented in the thesis focuses on the design and evaluation of a FSS based fractal antenna.

The work carried out in each chapter is highlighted in the proceeding subsection

7.1 CONCLUSION:

- Chapter 1 presents the overview of RF and microwave communication and also highlights the objectives of the research work.
- Chapter 2 deals with the literature review done in the fields of fractal MSA, Fractal MIMO arrays and FSS based antennas
- Chapter 3 deals with designing a single feed antenna with aperture coupling and then designing a sierpinski gasket fractal antenna with the same feeding method. . Then the same antenna is converted into 2x2 MIMO to check the envelope correlation coefficient and diversity gain. This chapter presented the theoretical analysis of a simple rectangular patch and then those concepts are used to design a single band MSA. The designed antenna shows a bandwidth of 139.4 MHz from 2.5.34 GHz to 2.364 GHz thereby allowing the antenna to be suitable for WLAN applications. In the same chapter a compact sierpinski gasket microstip antenna array is presented for IEEE 802.11, C-band and for STM band applications. The proposed antenna array shows an ultra-wide band performance of 1.006 GHz from 5.4832 GHz to 6.4892 GHz, as a result making it suitable for WLAN band from 5.75-5.856 GHz, STM band from 6-6.17 GHz and C-band from 5.850-6.425 GHz. Antenna shows an average

gain of 4.14dB over entire band of operation that suits short range applications. A low correlation coefficient of ECC<0.002 allows the he two antennas to be uncoupled when used for WLAN MIMO applications, thereby not providing interference to each other. The antenna has a high diversity gain of 9.99dB which allows the antennas to give good output when used in a 2 X 2 configuration at even low power.

- The next chapter 4 presents a compact hexagonal microstrip antenna array for IEEE 802.11, X-band wireless applications. The proposed antenna shows a dual band behavior for frequencies between (5.139-5.274) GHz and (8.71-9.44) GHz. Antenna shows an average gain of 4.14dB over entire band of operation that suits short range applications. A low correlation coefficient of ECC<0.0034 allows the two antennas to be uncoupled when used for WLAN MIMO applications, thereby not providing interference to each other. The antenna has high diversity gain which is prime requirement of a MIMO system to support high data rate applications.
- Chapter 5 presents a FSS (frequency selective surface) based antenna with a dual band at resonant frequency of 3.7 GHz and 7 GHz and having a band notch property from 7.8 GHz to 10.3 GHz. The antenna shows frequency selective properties and it is made from eight triangular sierpinski gasket fractals that are joined at the apex with a dipole. The proposed antenna shows an impedance bandwidth of 79.4 MHz and 1.439 GHz for the bands (3.7564-3.679) GHz and (7.8738-6.4348) GHz It is suits the wireless applications of WLAN and Wi-MAX.
- Chapter 6 presents the fabrication and testing of a sierpinski gasket fractal antenna array and a FSS based antenna for MIMO wireless applications and WLAN and X-band applications respectively. The simulated and measured results are seen to match closely.

Table 7.1 concludes the results of all the design, simulated, fabricated and tested antennas presented in this research work in this thesis report.

S. No.	**Antenna Design**	**Simulated Results**				**Measured**			
		Return freq (GHz)	Return loss (dB)	Impedance bandwidth (MHz)	Wireless Applica-tion	Resonant freq (GHz)	Return loss (dB)	Impedance bandwidth (MHz)	Wireless Application
1.	Conventional MSA	2.4	-37	139.4	IEEE 802.11	-	-	-	-
2	Sierpinski gasket fractal MSA	5.66	-39	1100	WLAN and C-band	-	-	-	-

S. No.	Antenna Design	Simulated Results				Measured			
		Return freq (GHz)	Return loss (dB)	Impedance bandwidth (MHz)	Wireless Applica-tion	Resonant freq (GHz)	Return loss (dB)	Impedance bandwidth (MHz)	Wireless Application
3.	2x2 Sierpinski gasket fractal MSA	5.62	-45	1006	WLAN and C-band	5.7,5.9, 6.4 5.8, 6.4, 6.8	-14, -14, -15 -16, -24, -15	200, 300 100, 100, 50	WLAN and C-band
4.	Hexagonal patch antenna with DGS	5.2, 9	-27, -15	241.1, 981.2	WLAN and X-band	-	-	-	-
5.	2x2 Hexagonal patch antenna with DGS	5.2, 9	-14, -15	135, 728	WLAN and X-band	-	-	-	-
6.	FSS based aperture coupled antenna	3.7, 7	-25, -25	77.4, 1439	WLAN, C-band and X-band	4, 6.1, 7.1	-35, -25, -27	100, 25000	WLAN, C-band and X-band

Apart from the research work presented in this thesis, a lot of work can be carried out in the future too. This is mentioned in the proceeding subsection.

7.2 FUTURE WORK

- Smart Antennas: These antennas work on the principle of DOA (direction of arrival). They only radiates in the direction of the user, therefore the antenna main lobe is in that specific direction with minimum interference. They contains DSP processors which handles the multiple antennas to focus their radiation to a specific user. Thus MEMS based smart antennas can also be designed for future use
- Electromagnetic Band Gap Structure (EBG): It has a 3D structure capable of trapping surface wave. So, it can create stop band by not allowing wave to propagate for some frequency range. It is very useful as it offers less interference. The designed fractal antennas can be incorporated with EBG structures to provide specific pass bands and stop bands to the antenna while operation.
- Patch Antennas with Switchable Slots: Microstrip patch antennas with switchable slots have attractive features like simple structure, single feed, and single layer design; this makes them compatible for wireless communication systems. Dual frequency can be realized by employing patch antenna with one switchable slot while when conventional patch antenna

with circular polarization is utilized with two switchable slots can be used to achieve dual band with circular polarization. It can also be employed in patch antennas to have switchable polarization i.e. Right Hand Circular Polarization (RHCP), and Left Hand Circular Polarization (RHCP). For example PASS was employed in the antenna used for MARS rover mission. These types of antennas can also be worked upon in future in coordination with fractal antennas.

- Massive MIMO: It is a technique in which more than 100 transmitting antenna is used to transmit the data. So, the error of probability is decreased, high quality signal is obtained with higher data rate and higher link performance. Therefore instead of designing just 2 MSA on a single substrate, massive MIMO can be designed which show better performance in terms of SNR improvement.

REFERENCES

[1] Goldsmith A. *Wireless Communication*, Cambridge University Press, 2005.

[2] Balanis CA. *Antenna Theory: Analysis and Design*, USA: John Wiley & Sons Incorporation, 1997.

[3] Goldsmith A. *Wireless Communication*, UK: Cambridge University Press, 2005.

[4] Jindal N. (2008). Antenna combining for the MIMO downlink channel. *IEEE Transactions on Wireless Communications*, 7(10), 3834-3844.

[5] Sainati RA. *CAD Of Microstrip Antennas For Wireless Applications*. Artech House, Incorporation, 1996.

[6] Jung W and De-Flaviis F (2004, June). A dual-band antenna for WLAN applications by double rectangular patch with 4-bridges. In *Antennas and Propagation Society International Symposium* (pp. 4280-4283).

[7] Jordan EC and Balmain KG. *Electromagnetic Waves and Radiating Systems*. India: Prentice Hall of India (PHI), 2001.

[8] Petros *et al.* (2003). Reviewing SDARS antenna requirements. *Microwaves & RF*, 42(9), 51-62.

[9] Gianvittorio JP and Rahmat-Samii Y (2002). Fractal antennas: A novel antenna miniaturization technique, and applications. *IEEE Antennas and Propagation magazine*, 44(1), 20-36.

[10] Siakavara K and Nasimuddin N. *Microstrip Antennas*. "Chapter-9", In Tech, April 2011.

[11] Werner DH and Ganguly S (2003). An overview of fractal antenna engineering research. *IEEE Antennas and propagation Magazine*, 45(1), 38-57.

[12] Kitlinski M and Kieda R (2004). Compact CPW-fed Sierpinski fractal monopole antenna. *Electronics Letters*, 40(22), 1387-1388.

[13] Yadav S *et al.* (2014, April). Koch curve fractal antenna for Wi-MAX and C-Band wireless applications. In *Communications and Signal Processing (ICCSP), 2014 International Conference on* (pp. 716-719). IEEE.

[14] Tang PW and Wahid PF (2004). Hexagonal fractal multiband antenna. *IEEE antennas and wireless propagation letters*, 3(1), 111-112.

[15] Kaur S and Khanna R (2015). Design and analysis of stair-shape UWB antenna with flowery DGS. *International Journal of Microwave and Wireless Technologies*, 7(1), 53-60.

[16] Kaur A, Khanna R, and Kartikeyan MV (2015). A stacked sierpinski gasket fractal antenna

with a defected ground structure for UWB/WLAN/RADIO astronomy/STM Link applications. *Microwave and Optical Technology Letters*, 57(12), 2786-2792.

[17] Islam MT *et al.* (2016). A compact slotted patch antenna for ultrawideband application. In *Computer and Information Technology (ICCIT), 2016 19th International Conference on* (pp. 76-79). IEEE.

[18] Mumin AO *et al.* (2015, April). Assessment of microstrip patch antenna performance based on dielectric substrate. In *Computer, Communications, and Control Technology (I4CT), 2015 International Conference on* (pp. 468-471). IEEE

[19] Khan M *et al.* (2015, July). UWB L-probe proximity fed V-slot patch antenna for early detection of breast cancer. In *Antennas and Propagation & USNC/URSI National Radio Science Meeting, 2015 IEEE International Symposium on* (pp. 1882-1883). IEEE.

[20] Sethi WT *et al.* (2016, December). Design of dual polarized hybrid LTCC antenna for UWB RFID applications. In *Electronic Devices, Systems and Applications (ICEDSA), 2016 5th International Conference on* (pp. 1-4). IEEE.

[21] Sze JY, Hsu CIG and Shiu JY (2008). Small CPW-fed band-notched ultrawideband rectangular aperture antenna. *IEEE Antennas and Wireless Propagation Letters*, 7, 513-516.

[22] Gatea KM (2012, November). Compact ultra-wideband circular patch microstrip antenna. In *Engineering Sciences (FNCES), 2012 First National Conference for* (pp. 1-5). IEEE.

[23] Darimireddy NK, Reddy RR and Prasad AM (2018). A Miniaturized Hexagonal-Triangular Fractal Antenna for Wide-Band Applications [Antenna Applications Corner]. *IEEE Antennas and Propagation Magazine*, 60(2), 104-110.

[24] Anguera J *et al.* (2017). High-directivity microstrip antenna with Mandelbrot fractal boundary. *IET Microwaves, Antennas & Propagation*, 12(4), 569-575.

[25] El-Khamy SE, Eltrass AS and El-Sayed HF (2017). Design of thinned fractal antenna arrays for adaptive beam forming and sidelobe reduction. *IET Microwaves, Antennas & Propagation*, 12(3), 435-441.

[26] Wang F *et al.* (2017). A compact UHF antenna based on complementary fractal technique. *IEEE Access*, 5, 21118-21125.

[27] Gorai A, Pal M and Ghatak R (2017). A Compact Fractal-Shaped Antenna for Ultrawideband and Bluetooth Wireless Systems With WLAN Rejection Functionality. *IEEE Antennas and Wireless Propagation Letters*, 16, 2163-2166.

[28] Choukiker YK and Behera SK (2017). Wideband frequency reconfigurable Koch snowflake fractal antenna. *IET Microwaves, Antennas & Propagation*, 11(2), 203-208.

[29] Eichler J *et al.* (2011). Design of a dual-band orthogonally polarized L-probe-fed fractal patch antenna using modal methods. *IEEE Antennas and Wireless Propagation Letters*, 10, 1389-1392.

[30] Hwang KC (2009). Dual-wideband monopole antenna using a modified half-Sierpinski fractal gasket. *Electronics letters*, 45(10), 487-489.

[31] Romeu J and Soler J (2001). Generalized Sierpinski fractal multiband antenna. *IEEE Transactions on Antennas and Propagation*, 49(8), 1237-1239.

[32] Ghatak R, Chatterjee S and Poddar DR (2012). Wideband fractal shaped slot antenna for X-band application. *Electronics letters*, 48(4), 198-199.

[33] Singhal S and Singh AK (2016). CPW-fed hexagonal Sierpinski super wideband fractal antenna. *IET Microwaves, Antennas & Propagation*, 10(15), 1701-1707

[34] Tripathi S, Mohan A and Yadav S (2014). Hexagonal fractal ultra-wideband antenna using Koch geometry with bandwidth enhancement. *IET Microwaves, Antennas & Propagation*, 8(15), 1445-1450.

[35] Wei K *et al.* (2017). A New Technique to Design Circularly Polarized Microstrip Antenna by Fractal Defected Ground Structure. *IEEE Transactions on Antennas and Propagation*, 65(7), 3721-3725.

[36] Singhal S and Singh AK (2016). CPW-fed octagonal super-wideband fractal antenna with defected ground structure. *IET Microwaves, Antennas & Propagation*, 11(3), 370-377.

[37] Kuzu S and Akcam N (2017). Array antenna using defected ground structure shaped with fractal form generated by apollonius circle. *IEEE Antennas and Wireless Propagation Letters*, 16, 1020-1023.

[38] Upadhyay D, Acharya I and Gupta AK (2015, April). DGS & DMS based hexagonal fractal antenna for UWB applications. In *Communications and Signal Processing (ICCSP), 2015 International Conference on* (pp. 0176-0179). IEEE.

[39] Nagpal A, Dillon SS and Marwaha A (2013, September). Multiband E-shaped fractal microstrip patch antenna with DGS for wireless applications. In *Computational Intelligence and Communication Networks (CICN), 2013 5th International Conference on* (pp. 22-26). IEEE.

[40] Ismail K and Anis KA (2014, August). Sierpinski Gasket fractal antenna with ring-shape defected ground structure for RFID application. In *Technology, Informatics, Management, Engineering, and Environment (TIME-E), 2014 2nd International Conference on* (pp. 340-344). IEEE.

[41] Colín-Beltrán E *et al.* (2013). Circular aperture slot antenna with common-mode rejection

filter based on defected ground structures for broad band. *IEEE Transactions on Antennas and Propagation*, 61(5), 2425-2431.

[42] Bashiri M *et al.* (2017). WiMAX, WLAN, and X-Band Filtering Mechanism: Simple-Structured Triple-Band Frequency Selective Surface. *IEEE Antennas and Wireless Propagation Letters*, 16, 3245-3248.

[43] Chatterjee A and Parui SK (2018). Beamwidth Control of Omni-directional Antenna Using Conformal Frequency Selective Surface of Different Curvatures. *IEEE Transactions on Antennas and Propagation*, 66(6) 2018.

[44] Li H *et al.* (2018). An Improved Multifunctional Active Frequency Selective Surface. *IEEE Transactions on Antennas and Propagation*, 66(4), 1854-1862.

[45] Taghizadeh M and Maddahali M (2017). New class of frequency selective surface based on non-resonant elements with high stability. *IET Microwaves, Antennas & Propagation*, 12(3), 406-409.

[46] Li JS, Li Y and Zhang L (2018). Terahertz Bandpass Filter Based on Frequency Selective Surface. *IEEE Photonics Technology Letters*, 30(3), 238-241.

[47] Yang S *et al.* (2017). Design of ultra-thin closely spaced dual-band bandpass frequency selective surface. *Electronics Letters*, 53(24), 1583-1585.

[48] Hua B, He X and Yang Y (2017). Polarisation-independent UWB frequency selective surface based on 2.5 D miniaturised hexagonal ring. *Electronics Letters*, 53(23), 1502-1504.

[49] Liu N *et al.* (2017). A Design Method for Synthesizing Wideband Band-Stop FSS via Its Equivalent Circuit Model. *IEEE Antennas and Wireless Propagation Letters*, 16, 2721-2725.

[50] Wu TK (1994). Cassini frequency selective surface development. *Journal of electromagnetic waves and applications*, 8(12), 1547-1561.

LIST OF PUBLICATIONS

Communicated to

- Singh J and Kaur A, Design of a hexagonal antenna array for MIMO WLAN application, *int. J. Bentham* Sci. 2018

- Singh J and Kaur A, Design of an aperture coupled sierpinski gasket fractal antenna for MIMO WLAN application, in Proc. ICIEEE, Delhi, India 2018